Quaternary Science Reviews 254 (2021) 106795

Contents lists available at ScienceDirect

Quaternary Science Reviews

journal homepage: www.elsevier.com/locate/quascirev

Late Neanderthal subsistence strategies and cultural traditions in the northern Iberia Peninsula: Insights from Prado Vargas, Burgos, Spain

Marta Navazo Ruiz [a, *], Alfonso Benito-Calvo [b], Rodrigo Alonso-Alcalde [c], Pedro Alonso [a], Héctor de la Fuente [a], Marta Santamaría [a], Claudia Santamaría [a], Adrián Álvarez-Vena [d], Lee J. Arnold [e], Ma José Iriarte-Chiapusso [f, g], Martina Demuro [e], Marina Lozano [h, i], José Eugenio Ortiz [j], Trinidad Torres [j]

[a] Área de Prehistoria. Facultad de Humanidades y Comunicación, Universidad de Burgos. Paseo Comendadores s/n., 09001, Burgos, Spain
[b] Centro Nacional de Investigación en Evolución Humana (CENIEH), Paseo Sierra de Atapuerca 3, 09002, Burgos, Spain
[c] Museo de Evolución Humana, Junta de Castilla y León, Paseo Sierra de Atapuerca nº 2, 09002, Burgos, Spain
[d] Departamento de Geología, Universidad de Oviedo, C/ Jesús Arias de Velasco s/n., E-33005, Oviedo, Spain
[e] School of Physical Sciences, Environment Institute, and Institute for Photonics and Advanced Sensing (IPAS), University of Adelaide, North Terrace Campus, 5005, Adelaide, SA, Australia
[f] Consolidated Research Team in Prehistory (IT-1223-19), Dpto. Geografía, Prehistoria y Arqueología, University of the Basque Country (UPV/EHU), c/ Tomás y Valiente s/n, 01006, Vitoria, Spain
[g] IKERBASQUE, Basque Foundation for Science, 48011, Bilbao, Spain
[h] Institut Català de Paleoecologia Humana i Evolució Social (IPHES), Zona Educacional 4, Campus Sescelades URV (Edifici W3), 43007, Tarragona, Spain
[i] Universitat Rovira i Virgili, Departament d'Història i Història de l'Art, Avinguda de Catalunya 35, 43002, Tarragona, Spain
[j] Laboratory of Biomolecular Stratigraphy, E.T.S.I. Minas y Energía, Universidad Politécnica de Madrid, C/ Ríos Rosas 21, Madrid, 28003, Spain

ARTICLE INFO

Article history:
Received 8 September 2020
Received in revised form
14 December 2020
Accepted 3 January 2021
Available online 29 January 2021

Handling Editor: Danielle Schreve

Keywords:
Neanderthal
Mousterian
Prado Vargas
Subsistence strategies
Technology
Chronological data
Bone retouchers

ABSTRACT

In order to better understand the causes and geographic patterns of Neanderthal demise it is necessary to broaden the focus of existing Neanderthal studies to include new sites from understudied regions, particularly those containing multi-level fossil and lithic records, and to improve regional-scale Neanderthal extinction frameworks using multiple dating techniques. To this end, we present an interdisciplinary study of the stratigraphy, chronology, pollen, fauna, lithic technology and human remains of the last Neanderthal level (Level N4) of Prado Vargas – a cave in northern Iberia, whose geographic location and chronology are ideal for investigating possible socio-economic and climatic influences on Neanderthal decline. Level N4 has yielded a rich Late Mousterian palimpsest indicative of repeated seasonal occupations, as well as a deciduous Neanderthal tooth, confirming the presence of children at the site. A wide range of human activities are detected in Level 4, with subsistence strategies demonstrating knowledgeable exploitation of the natural environs around the area. The site provides evidence for a distinctive recycling economy, including bone retouchers, recycling of cores, and intense (re)use of raw materials, which may reflect recurrent occupations or the particular cultural traditions of a regional group. Level N4 is dated to between 54.7 and 39.8 thousand years ago (ka) according to our new OSL and radiocarbon study. The late Neanderthal inhabitants of Prado Vargas were cold-adapted, and may have already been living in small, separate groups with marked territories and cultural traditions prior to the arrival of *Homo sapiens* in the Iberia Peninsula.

1. Introduction

The relationship between *Homo neanderthalensis* and *Homo sapiens* has been debated ever since its recognition as an extinct species in 1864. Early research into Neanderthals, particularly during the 1910s and 1920s, emphasised a perceived inferiority to *H. sapiens*. However, from the 1930s onwards this perception began to change and has continued to gain momentum over recent years with the advent of genetic research, better dating techniques and new approaches to the analysis of fossil anatomy (Harvati-

* Corresponding author.
E-mail address: mnavazo@ubu.es (M.N. Ruiz).

https://doi.org/10.1016/j.quascirev.2021.106795
0277-3791/

Papatheodorou, 2013). *H. neanderthalensis* is now widely considered to have evolved from an European Middle Pleistocene population. The appearance of characteristic Neanderthal anatomy is evident by around 200 thousand years ago (ka), with some researchers claiming that, from a cladistic point of view, most, if not all, of the European hominin fossil material that post-dates Marine Isotope Stage (MIS) 11 should invariably be assigned to *H. neanderthalensis* (Hublin, 2013). Late Neanderthals between 70 and 30 ka are considered to be a European lineage, although their geographical range was wider, reaching into Asia, to the east of Uzbekistan and even into Siberia (Krause et al., 2007).

The above mentioned Neanderthal anatomy appears to reflect gradual adaptations of successive European Middle Pleistocene populations to cyclical glacial-interglacial climate regimes. During peak cold periods, these populations migrated to refugia in the south of the continent in search of less adverse microclimates, and thus broke up into small groups that were mutually isolated. The archaeological record of late surviving Neanderthals suggests that they gradually waned across a broad geographic area, with the last known Neanderthal in the east, for example, found in Amud Cave, Israel (53.8 ka; (Villa and Roebroeks, 2014). In Europe, the last Neanderthals records are from Spy (Belgium) with disputed AMS radiocarbon (^{14}C) chronologies ranging between 36.9- 38.5 and 37.3–40.5 ka cal BP. The most securely dated late Neanderthal fossils in Europe come from Mezmaiskaya Cave, northern Caucasus (41 ka cal BP) (Pinhasi et al., 2011), along with Vindija, Croatia (44-40 ka cal BP; Deviese et al., 2017), Saint Cesare (41.9–40.6 ka cal BP; Hublin et al., 2012) and Arcy-sur-Cure (Grotte du Renne) with ages of 44 to 41 ka cal BP (Villa and Roebroeks, 2014).

The Iberian Peninsula provides evidence for potentially prolonged survival of Neanderthal populations at sites like Zafarraya, which includes several ages younger than 35 ka (Level I-3/7: 29.8 ± 0.6 ka; C-1 Level I-3/7: 28.9 ± 4.2 ka and 34.0 ± 0.5 ka; Hublin et al., 1995). Other sites in the south of the Peninsula, such as Cueva Antón and Carihuela have yielded relatively recent ages of 37.1 and 30.4 ka cal. BP, respectively, for layers associated with Mousterian lithic assemblages (Zilhão et al., 2017; Carrión et al., 2019).

The Neanderthal extinction can now be dated to a period in the 41-39 ka cal BP range (Higham et al., 2014). Anatomically modern humans (AMH) spread across Eurasia between 60 ka and 50 ka (Villa and Roebroeks, 2014). The oldest dated AMH remains from Europe are represented by ZooMS-identified bone fragments from Bacho Kiro (Bulgaria), with 95.4% calibrated ^{14}C ranges of 46.8 to 42.8 ka cal. BP (Hublin et al., 2020), as well as fossils from Pestera cu Oase (Romania), dated to 42-37 ka (Trinkaus et al., 2003). For some regions, different authors claim that the most recent Neanderthal ages do not coincide with the oldest *H. sapiens* ages, and that Neanderthals became extinct before *H. sapiens* reached Western Europe, making coexistence between the two species difficult. However, coexistence and hybridisation is known to have taken place in the Near and Middle East (Pinhasi et al., 2011), and recently published genetic evidence from the Denisova 11 individual demonstrates a late Pleistocene Neanderthal migration from west to east Eurasia, as well as admixture with denisovan groups (Slon et al., 2018).

Much has been written about the decline of the Neanderthals and the arrival of modern humans, with many interpretations suggesting, directly or indirectly, that inferiority was a factor in the disappearance of the former. The key question is whether Neanderthals, who had lived in Europe for tens of thousands of years and survived multiple ice ages, became extinct due to internal changes and population shifts, or the arrival of *H. sapiens*. Some DNA evidence suggests that genetically, Neanderthals exhibited similar traits to other species at the peak of a demographic crisis, which could and were therefore have potentially condemned them to extinction (Lalueza, 2020). In order to better constrain these phylogeographic histories, it is necessary to broaden the focus of Neanderthal studies beyond just the last surviving records – targeting new sites with multi-level fossil and lithic records that extend beyond the arrival of *H. sapiens*, and within which Neanderthal bottlenecks and populations changes might be detected.

The present study aims to present new datasets that could help inform both of these debates. We present a new archaeostratigraphic and chronological record from the cave site of Prado Vargas, which includes several well-preserved occupation levels that offer insights into how the penultimate and final Neanderthal groups lived. We focus on the excavated record of Level N4, which includes human remains and a detailed lithic assemblage indicative of subsistence strategies and cultural traditions adopted by local Neanderthal groups.

2. Regional setting

Prado Vargas is part of the Ojo Guareña multilevel cave complex in the Cantabrian Range (northern Spain) (Fig. 1). These caves developed in the north flank of a syncline by the dissolution of Late Cretaceous limestones and dolomites (del Olmo Zamora, 1978). Ojo Guareña is formed by eight cave levels, ranging between relative heights of +230 m and +0 m above the current drainage network (Ortega and Martín, 2013). The Prado Vargas cave is a 120 m-long sub-horizontal passage on the sixth level of the karst complex, and has been shaped by an old karst spring that drains into the Trema River valley. Prado Vargas represents the oldest known archaeological site in the complex, and was opened by Trinidad Torres in 1986 while digging several test pits in search of *Ursus spelaeus*. A 4 m^2 area was originally dug at the entrance, which unearthed a Mousterian level (N4). In 2006, another small dig was undertaken to extend the original excavation by a further 4 m^2. Neither operation was extended into or below Level N4, hence the existence of additional stratigraphic levels remained unknown. In 2016, our interdisciplinary team began a new study aimed at expanding the excavation area and defining the complete archaeo-stratigraphic record, focusing primarily on Level N4. The results of our ongoing fieldwork campaign are outlined in the present study.

A preliminary chronological assessment of Prado Vargas Level N4 was presented by Navazo et al. (2005) based on amino acid racemisation (AAR) dating of a single horse tooth (sample BSL 4682). The aspartic acid D/L ratio of this tooth was compared with results obtained on similar mammal teeth from other Iberian sites that had been independently dated using 14C, U/Th and electron spin resonance (ESR). Using this regional calibration dataset, an age of 46.4 ka (with no assigned uncertainty) was calculated for the horse tooth from Level N4. This preliminary age suggests that Prado Vargas was occupied by Neanderthal populations in the millennia leading up to their regional demise. As part of the present study we have sought to expand this preliminary chronological framework using different types of samples and complementary dating techniques.

3. Material and methods

A multidisciplinary approach has been used to investigate the Level N4 archaeological record, including a detailed study of the stratigraphy, chronology, pollen, faunal remains, lithic assemblage and a Neanderthal tooth.

3.1. Stratigraphy

The new stratigraphic study of the Prado Vargas deposit is based on a detailed description and mapping of the entire accessible

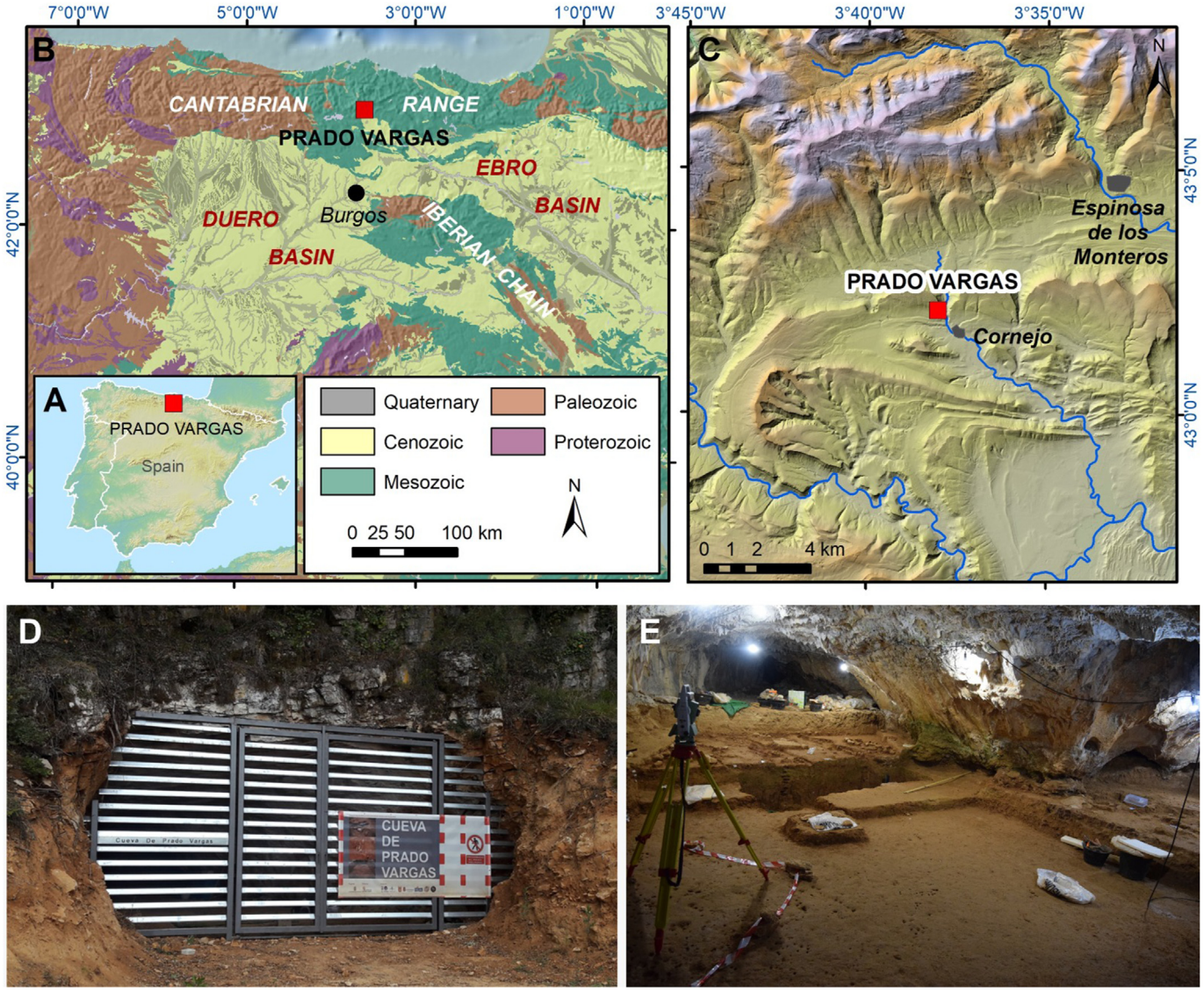

Fig. 1. Situation of Prado Vargas site. A) Iberian Peninsula. B) General geological situation. C) Topographic situation. D) Prado Vargas cave entrance. C) Prado Vargas excavation.

section of the site, and has been complemented with stratigraphic data from a geological drill used to ascertain the depth of the sedimentary infill. To map and integrate these data, we have used a GNSS RTK Leica GS015 device, a Faro Focus 3D X330 laser scanner and photogrammetry (Agisoft Metashape) to generate 3D models and orthoimages of the stratigraphic section with millimetre resolution. The stratigraphic models have been georeferenced using the local coordinates of the dig and digitized with ArcGIS.

3.2. Numerical dating

3.2.1. Optically stimulated luminescence (OSL)

Two single-grain OSL dating samples (PRA19-1 and PRA19-2) were collected from the Level N4 in square H32 to provide replicate estimates of when sedimentary quartz grains were last exposed to light prior to burial. The OSL samples were taken from the same vertical depths in Unit IV and from within a 40 cm lateral distance of each other. Both samples were collected from cleaned exposure faces using opaque PVC tubes, and were immediately sealed with light-proof plastic upon extraction. Approximately 500 g of additional bulk sediment was collected from material directly surrounding each sample for dosimetry and water content assessments.

Quartz grains were processed under safe light conditions (dim red LEDs) at the University of Adelaide using standard preparation procedures (e.g., Demuro et al., 2013), including a 48% hydrofluoric acid etch (40 min) to remove the alphairradiated outer layers of the quartz extracts. OSL measurements were made using the experimental apparatus described by Arnold et al. (2013, Arnold et al., 2016a, and further detailed in the Supplementary Information. Purified quartz grains with a diameter of 212–250 μm were manually loaded onto aluminium discs drilled with an array of 300 × 300 μm holes to ensure true single-grain resolution during equivalent dose (D_e) evaluation (Arnold et al., 2012). Individual D_e values were determined using the single-aliquot regenerative-dose (SAR) procedure (Murray and Wintle, 2000) shown in Table S1, which yielded suitable multiple-grain aliquot and single-grain dose-recovery test results for sample PRA19-2 (Figure S1). Between 2500 and 3000 single-grain D_e measurements were made for each sample (Table S2), with individual D_e values being included in the final age calculation if they satisfied a series of standard and widely tested quality-assurance criteria, as detailed in the

Supplementary Information. Sensitivity-corrected dose-response curves were constructed using the first 0.08 s of each OSL stimulation after subtracting a mean background count obtained from the last 0.25 s of the signal (Figure S2).

The environmental dose rate for the OSL samples was estimated using a combination of *in situ* field gamma spectrometry and low level beta counting, taking into account cosmic ray contributions (Prescott and Hutton, 1994), an assumed minor internal alpha dose rate (Bowler et al., 2003), beta-dose attenuation and long-term water content, as detailed in Table 1 and the Supplementary Information.

3.2.2. Radiocarbon dating

Two charcoal samples from Level 4 were selected for AMS ^{14}C dating, which was performed at BETA Analytic Inc. These samples were collected from the middle to lower layers of Level 4 in the north central sector of the current excavation. The ^{14}C samples were prepared using standard acid-base-acid pre-treatment with isotopic fractionation corrected for using measured ^{13}C values. The ^{14}C dating results have been calibrated with IntCal20 curve (Reimer et al., 2013) using OxCal 4.4 software (Bronk Ramsey, 2009).

3.2.3. Amino acid racemisation (AAR) dating

Samples of powdered dentine were obtained by drilling a hole 2 mm in diameter and 5–10 mm in depth with a thin diamond-headed device. To avoid contamination, powder from the outermost 1–2 mm part was rejected. Prior to protein hydrolysis and amino acid derivatization, the samples were treated to eliminate free amino acids (dialysis) following the dialysis step proposed by Lafont et al. (1984) and Marzin (1990). The powder sample (4.5–16.8 mg) was dissolved in 1 ml of 2N hydrochloric acid and sonicated. Following the addition of 5 ml of PBS buffer, the sample was dialyzed using 3500 Da (Spectra/Por mnco 3500) membrane for a period of 24 h in a buffered solution, with magnetic stirring at room temperature.

Samples were subjected to amino acid analysis using a high performance liquid chromatograph (HPLC) in the Biomolecular Stratigraphy Laboratory of Polytechnical University of Madrid, following the sample preparation protocol described by Kaufman and Manley (1998). The prepared solutions were injected into an Agilent-1100 HPLC equipped with a fluorescence detector, following Torres et al. (2014).

3.3. Pollen analysis

The palynological record of Level 4 was obtained from samples taken in two core sections: A (samples 14, 15 and 16) and C (samples 8, 9, and 10). The samples were processed using the classic physical–chemical method, and the sporo-pollen contents were identified and counted with optical microscopy (Burjachs et al., 2003).

3.4. Fauna

3.4.1. Microfauna

A total of 70 sediment samples (10–15 kg per sample) were water-screened using superimposed sieves with 2- and 0.5-mm mesh sizes. Fossil remains were picked out from the sieve residues with a binocular microscope under 10× magnification; taphonomic and taxonomic observations were carried out by means of a parallel-optics type stereo microscope Nikon SMZ800N equipped with a 5 Mpx digital camera and a drawing tube. The taxonomic identifications were from the cheek teeth, except for lagomorphs, which were from the postcranial skeleton.

The general identification of shrews and rodents followed Chaline (1972; 1974), and Román (2019). Taxonomic classification followed the systematics proposed by Wilson et al. (2016, 2017) for rodents, and Wilson and Mittermeier (2018) for shrews and moles. For a preliminary identification of the accumulating agent, small-mammal remains were scrutinised for alterations caused by predation, following Andrews (1990) and Fernández-Jalvo et al. (2016).

The habitat preferences of each species were obtained from Cuenca-Bescós et al. (2009, 2010), Wilson et al. (2016, 2017) and Wilson and Mittermeier (2018) and quantified with the habitat weighting method (Cuenca-Bescós et al., 2009). The climatic conditions in which Level 4 was formed were inferred by means of the Bioclimatic Model (Hernández-Fernández, 2001, 2001b; Hernández-Fernández and Peláez- Campomanes, 2005; Hernández-Fernández et al., 2007), and the results were compared with present-day data for the Prado Vargas location (MAT: 11.0 °C; MTW: 18.8 °C; MTC: 4.0 °C y MAP: 926 mm) according to the Iberian Climate Atlas (Couto et al., 2011) and its online GIS application (agroclimap.aemet.es).

3.4.2. Macrofauna

In total, 1156 macrofauna remains were studied. A zooarchaeological and taphonomic methodology (Lyman, 1994; Reitz and Wing, 1999) was employed for the faunal analysis of Level 4. NISP (Number of Identified Specimens), MNE (Minimum Number of Elements), MNI (Minimum Number of Individuals) and skeletal survival rate (Brain, 1981; Lyman, 1994) were calculated. Skeletal survival rate gauges the proportion between the elements recovered and those expected (Brain, 1969). For this calculation, the following formula was used: NE*100/number of element in the animal skeleton*MNI.

Taxonomically non-identifiable remains were classified using the five size categories described by Bunn (1986): very large (>1000 kg), large (300–1000 kg), medium (100,300 kg), small (20–100 kg) and very small (<20 kg). Age of death wasdefined following Barone (1976) and Azorit et al. (2002).

Cut mark classification followed the relevant literature (Shipman and Rose, 1983; Lyman 2008; Fernández-Jalvo and Andrews, 2016), and distinguished different types of cut marks following Binford (1981), Fisher (1995) Domínguez-Rodrigo (1997, 2002), Nilssen (2000) and Lyman (2008). Fracture classification followed the criteria established by Bunn (1983) and modified by Villa and Mahieu (1991).

Burnt remains were recorded, and colour change as a result of exposure time (Shipman et al., 1984), was classified following the criteria defined by Stiner et al. (1995), with degrees of cremation starting with Degree 0 as absence of alteration.

Carnivore identification and action was studied following Haynes (1980; 1983), Blumenschine (1995), Andrews and Jalvo (1997), Selvaggio and Wilder (2001), Domínguez-Rodrigo and Piqueras (2003), Yravedra (2004), Delaney-Rivera et al. (2009) and Fernandez-Jalvo and Andrews (2016).

3.5. Lithic assemblage

3.5.1. Raw materials

The study area was surveyed with the aid of a GPS to map the flint outcrops and analyse the location of raw material sources. The material was identified and characterized by microscopic analysis using a transmission light microscope, mass spectrometry geochemical analysis (ICP-MS) and X-Ray Diffraction (XRD) (Navazo et al. 2005, 2008).

3.5.2. Technology

The lithic assemblages were studied using the Logical Analytical System (LAS), (Carbonell et al., 1983, 1992; Rodríguez, 2004). The

Table 1
Dose rate data, single-grain equivalent doses and quartz OSL ages for the Prado Vargas samples.

Sample name	Grain size (μm)	Water content[a]	Environmental dose rate (Gy/ka)				Equivalent dose (D_e) data					OSL age (ka)[f,l,m]
			Beta dose rate[b,c]	Gamma dose rate[c,d]	Cosmic dose rate[e]	Total dose rate[c,f,g]	No. of grains[h]	Over-dispersion (%)[i]	Age Model[j]	L_{max} score[k]	D_e (Gy)[f]	
PRA19-1	212–250	21 ± 2	1.25 ± 0.06	0.82 ± 0.03	0.04 ± 0.01	2.13 ± 0.10	192/3000	29 ± 3	CAM	−92.85	116 ± 3	54.6 ± 3.2
									MAM-3	−90.91	100 ± 7	46.9 ± 4.2
									MAM-4	−88.72	103 ± 4	48.3 ± 3.2*
PRA19-2	212–250	21 ± 2	1.34 ± 0.07	0.81 ± 0.03	0.04 ± 0.01	2.22 ± 0.11	247/2500	26 ± 2	CAM	−120.98	110 ± 3	49.3 ± 2.8
									MAM-3	−118.39	103 ± 5	46.2 ± 3.2*
									MAM-4	−118.31	104 ± 6	46.8 ± 3.5

[a] Long-term water content, expressed as % of dry mass of mineral fraction, with an assigned relative uncertainty of ±10%.
[b] Beta dose rates were calculated on dried and powdered sediment samples using a Risø GM-25-5 low-level beta counter (Bøtter-Jensen and Mejdahl, 1988), after making allowance for beta dose attenuation due to grain-size effects and HF etching (Brennan, 2003).
[c] Specific activities and radionuclide concentrations have been converted to dose rates using the conversion factors given in Guérin et al. (2011), making allowance for beta-dose attenuation (Mejdahl, 1979; Brennan, 2003).
[d] Gamma dose rates were calculated from *in situ* measurements made at each sample position with a NaI:Tl detector, using the 'energy windows' approach (e.g., Arnold et al., 2012).
[e] Cosmic-ray dose rates were calculated using the approach of Prescott and Hutton (1994) and assigned a relative uncertainty of ±10%.
[f] Mean ± total uncertainty (68% confidence interval), calculated as the quadratic sum of the random and systematic uncertainties.
[g] Includes an internal dose rate of 0.03 Gy/ka with an assigned relative uncertainty of ±30%, based on intrinsic ^{238}U and ^{232}Th contents published by Mejdahl (1987), Bowler et al. (2003), Jacobs et al. (2006) and Pawley et al. (2008), and an a-value of 0.04 ± 0.01 (Rees-Jones, 1995; Rees-Jones and Tite, 1997).
[h] Number of D_e measurements that passed the SAR rejection criteria and were used for D_e determination/total number of grains analysed.
[i] The relative spread in the D_e dataset beyond that associated with the measurement uncertainties of individual D_e values, calculated using the central age model (Galbraith et al., 1999).
[j] Age model used to calculate the sample-averaged D_e value for each sample. CAM = central age model; MAM-3 = 3-parameter minimum age model; MAM-4 = 4-parameter minimum age model (Galbraith et al., 1999). MAM-3 and MAM-4 D_e estimates have been calculated after adding, in quadrature, a relative error of 20% to each individual D_e measurement error to approximate the underlying dose overdispersion observed in 'ideal' (well-bleached and unmixed) sedimentary samples (e.g., global overdispersion dataset mean value of 20 ± 1% reported by Arnold and Roberts, 2009) and the minimum estimate of intrinsic (experimental) overdispersion determined from the single-grain dose-recovery test for sample PRA19-2.
[k] Maximum log likelihood score of the CAM, MAM-3 or MAM-4 fit. For a given sample, the L_{max} score of the MAM-3 is expected to be substantially higher (i.e. at least 1.92 greater) than that of the CAM when the addition of the extra model parameter improves the fit to the data. Likewise, the L_{max} score of the MAM-4 is expected to be significantly greater than that of the MAM-3 (by at least 1.92 when compared with the 95% C.I. of a X^2 distribution) when the addition of the extra model parameter improves the fit to the data. If the extra parameter of the MAM-3 (or MAM-4) is not supported by the data, then its L_{max} score will be similar to (i.e. within 1.92 of) the CAM (or MAM-3) L_{max} score, indicating that the simpler age model explains the data equally well (Arnold et al., 2009).
[l] Total uncertainty includes a systematic component of ±2% associated with laboratory beta-source calibration.
[m] The preferred age is indicated with an asterisk. For these samples, the preferred age has been derived using the statistical age model that yielded the optimum L_{max} score, following the criterion outlined in footnote[k] and Arnold et al. (2009).

LAS approaches the study of technological processes on the basis of the stage at which the objects were produced during the reduction sequence, striving to avoid fixed typological preconceptions. The LAS classifies objects into several structural categories, depending on their position in the production chain (Table 2, LAS categories). In this study, 819 items are examined. Cores are studied following Vaquero et al. (2008) and Carmignani et al. (2017).

3.5.3. Traceology

Cretaceous flint samples were collected from secondary outcrops near Prado Vargas, in the Basque Cantabrian basin (43°02′00.7 "N 3°39′52.6 "W) (Navazo et al., 2005; Navazo and Díez, 2008; Vallejo et al., 2017) for an experiment in which ten tools with similar technological features to those found at the site were knapped by experts. Skinning, defleshing and dismembering (meat processing) was done on both forehind limbs of roe deer (*Capreolus capreolus*), which is present in the Prado Vargas record, while the long bones were also used for bone scraping. *Bos primigenius taurus* limbs were used for work on hides. Two wood species, *Quercus robur* and the softer *Ulmus minor*, were chosen on the basis of their different degrees of hardness.

The results from the experimental samples were compared with a small archaeological sample of 10 tools from Prado Vargas Level 4. These tools were analysed under a binocular microscope and then with a monitored Olympus LEXT OLS3100 confocal microscope.

3.5.4. Bone retouchers

Sixty eight bone retouchers were identified amongst the 1156 faunal remains from Level 4. Morphometric data were collected using a digital calliper to obtain the maximum length, width, and thickness of the bone fragments used as retouchers. When identifiable, the selected species and anatomic elements were recorded. Otherwise, an animal size class was estimated from the cortical thickness of the fragment (see 3.4.1. Macrofauna). The number of pits, scores, and scale removals were counted. The definition of the active areas and their fundamental characters and marks followed research by Mallye et al. (2012).

3.5.5. Human remains

One human tooth was found on Level 4 during the 2019 excavation season. Prior to analysis, the tooth was cleaned with demineralised water and ethanol to remove sediment adhered to different crown surfaces. This tooth was morphologically described following established anatomical terminology (Carlsen, 1987; Scott and Turner, 1997; Bailey, 2002). The assessment of its occlusal dental wear was based on Molnar (1971).

With this isolated tooth, we were only able to assess the age of tooth loss following Schour and Massler (1944). The bucco-lingual (BL) and mesio-distal (MD) diameters were measured directly on the tooth with digital sliding calipers and compared with data published for Neanderthals and *H. sapiens* samples (Upper

Table 2
Logic analytical system categories (LAS) (Santamaría et al., 2020).

Logical Analytical System	Common terms	L.A.S Subdivision Categories	Analysed variables
Natural Base (nB)	Pebbles, cobbles, hammers or selected blocks	nBa: Selected and transported bases nBb: Hammerstones with percussion marks nBc: Cobble fragments with or without percussion marks	Size, shape, weight and percussion marks
Exploitation First Generation Negative Base of exploitation (1GNBe) Second Generation Negative Base of exploitation (2GNBe)	Cores, cores on flakes.	1GNBe: exploitation of a pebble or block to obtain Positive Bases 2GNBe: positive base exploitation to obtain more Positive Bases (core on flake)	Volumetric concept, Striking platform organisation, exploitation methods, degree of symmetry and hierarchy, surface preparation angle. (Carbonell et al., 1999) (Carmignani et al., 2017) (Vaquero, 1999) (Vaquero and Carbonell, 2003) (Menéndez, 2009)
Positive base (PB)	Flakes and debris	Positive Bases (PB), products of exploitation (flakes)	The PB morphology. Direction of previous dorsal removals, angles between surfaces (Carbonell et al., 1999) (Carmignani et al., 2017)
Fragmented Positive Bases (FPB)	Broken flakes	Broken flakes; flakes with preserved point of percussion but incomplete margins	
Fragments of Positive Base (Frag of PB)	Flake fragments; flakes with absent butt		
Configuration First Generation Negative Base of configuration (1GNBc) Second Generation Negative Base of configuration (2GNBc)	Tools on pebble, tools on flakes	1GNBc: Tools on pebble, cobble or block 2GNBc: Tools on flakes	(Carbonell et al., 1999) Faciality, centripetal character, retouching angle, depth, mode, delineation, type (Laplace, 1972) Typology
Fragments (FRAG)	Angular fragments		
Indeterminate (INDET)	Unidentifiable lithic items		

Palaeolithic and recent) in Faerman et al. (1994), Mizoguchi (2002), Arnaud et al. (2016), Hershkovitz et al. (2016), and Trinkaus and Walker (2017).

4. Results

4.1. Stratigraphic sequence

The sequence preserved in the entrance of Prado Vargas Cave is composed of 9.3 m of sand, clay and gravel, divided into 9 lithostratigraphic units (Fig. 2). The uppermost units (PV1 and PV2) are only observed locally and seem to consist of rubble and a pit from a recent period. Unit PV3 consists of 45 cm of medium and fine-grain sands and laminated clayey sands with pale yellow colours. Speleothems are preserved on the upper surface of this unit (Fig. 2).

Unit PV4 (15–20 cm), which contains archaeological Level 4, is composed of a package of highly malleable reddish-toned clays, which locally contains sub-rounded limestone sand grains, subangular limestone pebbles and sporadic decimetric limestone fragments. To the east there are more subangular gravels found nearer the roof, while to the west, the matrix is more clayey. The ongoing excavation of this unit is beginning to reveal a more complex stratigraphy near the entrance zone, with layers of yellowish sand interspersed between the clay packages.

Unit PV5 (13 cm) is composed of clayey laminated sands and scattered gravels, located above a section of red clay (Fig. 2). Two units have been observed in the red clay section: PV6 and PV7. Levels PV6 and PV7 are 59–71 cm deep, sterile in the excavated area, and found where waterlogging and decanting processes are predominant. In the surveyed area, Unit PV8, which contains archaeological remains (archaeological Level N8), is composed of dark-coloured sand with a high proportion of organic matter, indicating the presence of combustion residue. Below Unit PV8 lies a section composed of gravels and yellowish sand layers, and a silty-clay matrix, with coarse stratification. These deposits, formed by fluvial dynamics, are identified as PV9. Scattered archaeological remains have also been found in this unit. 1.5 m of this deposit is currently visible, although the 2018 mechanical drill core showed that it continues downwards for a further 5 m. Below PV9 there is 25 cm of reddish clay lying above 1.2 m of limestone fragments; the latter overlies limestone, which is interpreted as the bedrock of the cave (Fig. 2).

4.2. Numerical dating

4.2.1. Optically stimulated luminescence (OSL)

Table 1 shows a summary of the environmental dose rates, single-grain D_e values and final ages obtained for the two OSL dating samples from Unit PV4. Between 6 and 10% of quartz grains measured per sample were considered suitable for OSL dating purposes after application of the SAR quality assurance criteria (Table S2), with the majority of measured grains (56–75%) being rejected from further consideration because they exhibited weak or no OSL signals. Representative OSL dose-response and decay curve for grains that passed the quality assurance criteria are shown in Figure S2. The characteristic saturation dose (D_0) values of these grains (calculated using a single saturating exponential dose-response curve fit) are high enough to enable finite D_e determination over the observed burial dose ranges for these samples (30–300 Gy), hence the single-grain burial dose estimates are not thought to have been negatively affected by dose saturation. To examine this formally, we applied the $2 \times D_0$ acceptance threshold criterion outlined by Demuro et al. (2015, 2019), which ensures that only grains with $2 \times D_0$ values higher than a specific burial dose are accepted for final D_e estimation. Progressively higher $2 \times D_0$ thresholds of 50–300 Gy (increasing in 50 Gy increments) were applied to the accepted D_e datasets, and the effects on weighted mean D_e were examined after taking into consideration associated

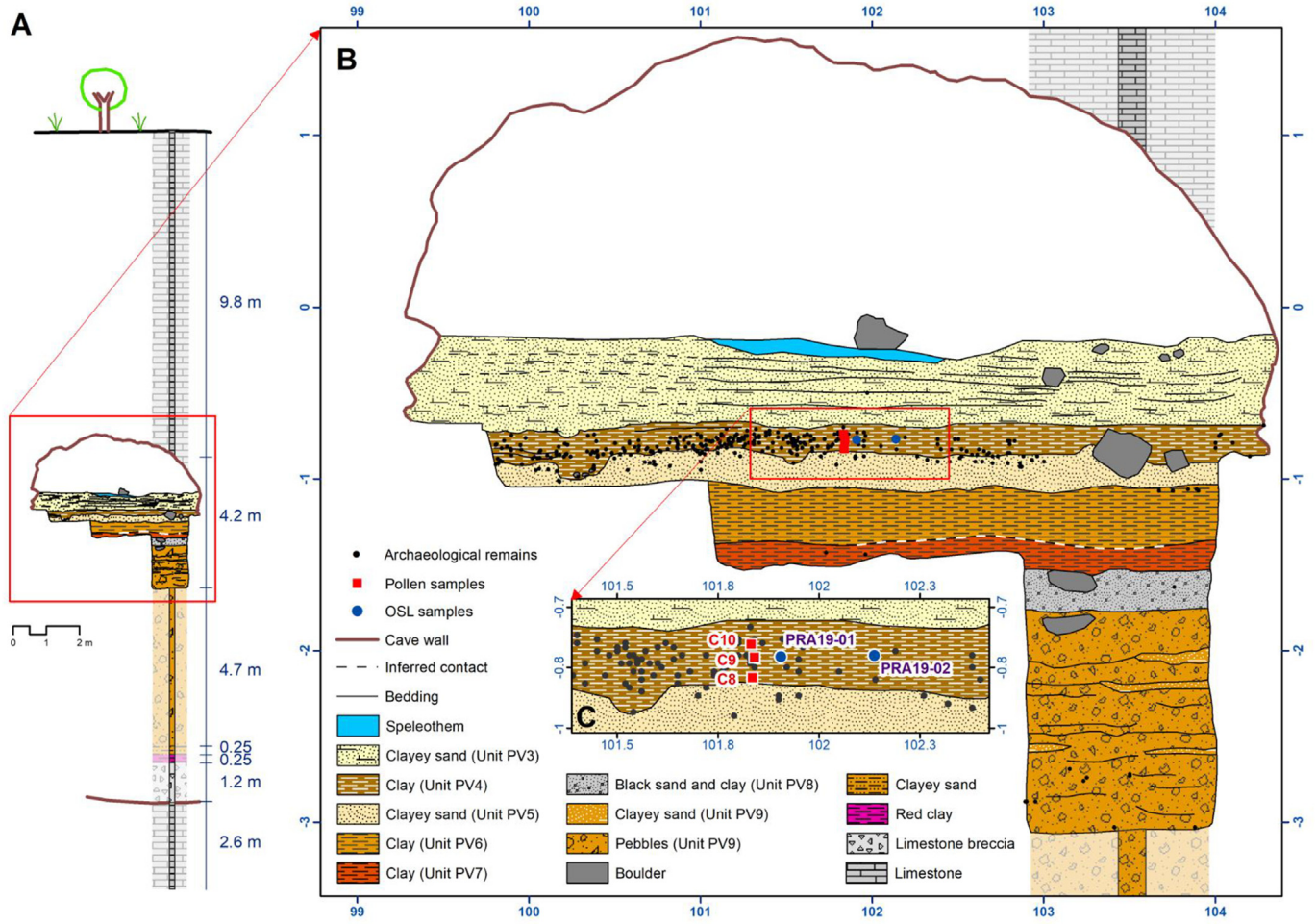

Fig. 2. Prado Vargas stratigraphic sequence. A) Geological drilling, B) Stratigraphic sequence in section X201; C) OSL and pollen samples collected at Level N4. Local coordinate grid, in m.

2σ uncertainty ranges (Arnold et al., 2016). For both the dose-recovery and natural D_e datasets, it was found that selecting grains with progressively higher D_0 values did not alter the weighted mean D_e value or overdispersion at 2σ (e.g., Fig. 3 c-d). These results support the interpretation that the single-grain OSL D_e values calculated using all accepted grains have not been adversely affected by dose-response curve saturation, at least over the observed burial dose ranges of 0–300 Gy.

The single-grain D_e distributions of grains that passed the SAR quality assurance criteria are shown as radial plots in Fig. 3 a-b. Both samples exhibit similar D_e distributions, characterised by moderate dose dispersion (relative D_e ranges of 2.3–2.6), discernible proportions of D_e values lying outside of the weighted mean (central age model; CAM) burial dose 2σ ranges, prominent D_e clusters around ~100 Gy, and tails of higher D_e values reaching up to ~300 Gy. The overdispersion values for these samples (26–29%) are broadly similar to those reported for some well-bleached and unmixed single-grain OSL D_e datasets at 2σ (e.g., Demuro et al., 2015; Arnold et al., 2016), though they are slightly higher than the average overdispersion of 20 ± 1% reported for ideal samples by Arnold and Roberts (2009) and they are significantly higher than the overdispersion value of 10 ± 4% obtained for the single-grain dose recovery test of sample PRA19-2 (Supplementary Information). Application of the maximum log likelihood (L_{max}) test (Arnold et al., 2009) indicates that either the three- or four-parameter minimum age models (MAM-3 or MAM-4) of Galbraith et al. (1999) are statistically favoured over the CAM for both D_e datasets (Table 1). These various D_e characteristics suggest that dose dispersion originating from field-related sources or intrinsic experimental sources not captured by the dose recovery test may have exerted a minor to moderate influence on the OSL samples.

We interpret these single-grain D_e datasets as primarily reflecting minor syn-depositional mixing of externally derived (well-bleached) sediments with older generations of pre-existing cave deposits during transportation through the cave system. Such complex karstic sedimentary processes have the potential to give rise to single-grain D_e distributions that are outwardly similar to those commonly reported for heterogeneously bleached single-grain OSL samples (e.g., Olley et al., 1999; Arnold et al., 2007, 2008), for which the MAM has been shown to yield suitable burial dose estimates for the most fully bleached (and undisturbed) grain populations (e.g. Galbraith et al., 1999; Bailey and Arnold, 2007; Arnold et al., 2009). Minor dose dispersion arising from intrinsic sources of D_e scatter (e.g., Demuro et al., 2013) or spatial variations in beta dose rates experienced by individual grains (e.g., Nathan et al., 2003) should not necessarily be ruled out at this site, although post-depositional mixing or bioturbation (e.g., Arnold et al., 2013) is not thought to have contributed significantly to the D_e datasets given the preservation of clear layering and stratigraphic boundaries.

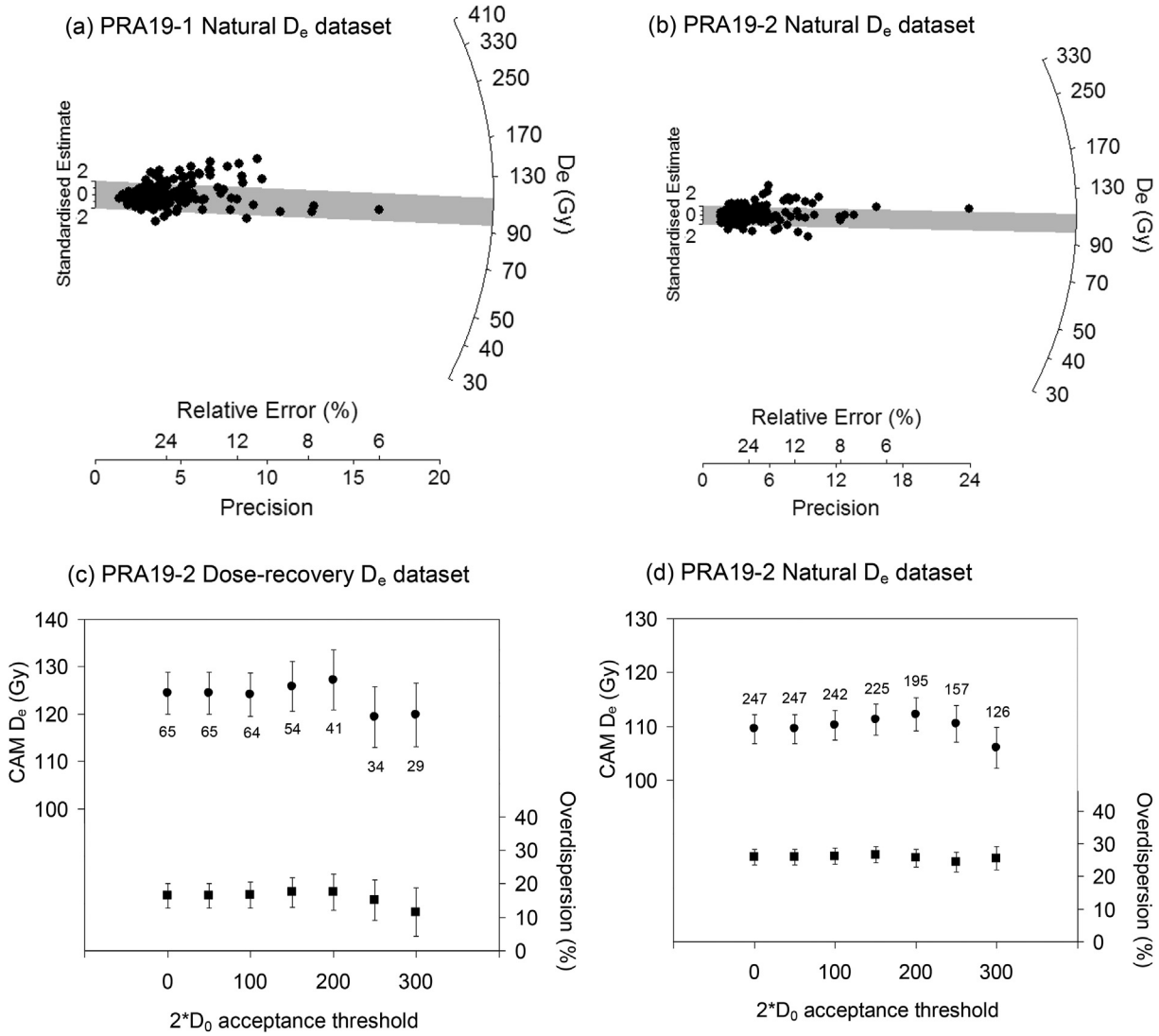

Fig. 3. (a)–(b) Single-grain OSL D_e distributions for the two OSL samples dated in this study, shown as radial plots. The grey bands are centred on the D_e values used for the age calculations, which were derived using either the 3-parameter minimum age model (sample PRA19-2) or the 4-parameter minimum age model (sample PRA19-1) of Galbraith et al. (1999). (c)–(d) Single-grain weighted mean (central age model; CAM) D_e and overdispersion values for the dose-recovery and natural D_e dataset of PRA19-2 after applying the $2 \times D_0$ acceptance threshold criterion of Demuro et al. (2015) (D_e errors are shown at 1σ). In these plots, progressively higher $2*D_0$ thresholds have been applied to the D_e datasets, starting with a $2*D_0$ threshold of 0 and increasing the $2*D_0$ threshold in increments of 50. In each instance, grains were only accepted for further D_e analysis if their individual $2*D_0$ value equalled or exceeded the corresponding threshold shown on the x-axis at 2σ (see Arnold et al., 2016a for details). The number of accepted grains remaining after applying progressively higher $2*D_0$ thresholds are shown for each dataset. 41.

On the basis of these D_e interpretations, we have opted to use the MAM to derive the burial dose estimates for the Prado Vargas OSL samples (Table 1). The decision of whether to use the MAM-3 or MAM-4 for the final age calculation of each sample has been made on statistical grounds using the L_{max} score, as outlined by Arnold et al. (2009). It is worth emphasising that the choice of age model does not have a statistically significant bearing on the final OSL interpretations as the CAM, MAM-3 and MAM-4 ages for each sample are indistinguishable at 1σ or 2σ. The final OSL ages for the two replicate samples overlap at 1σ, supporting the overall reliability of the OSL results. Both samples indicate that Unit PV4 was deposited in the cave around 46.2 ± 3.2 ka to 48.3 ± 3.2 ka (1σ uncertainty ranges), towards the middle of MIS 3.

4.2.2. Radiocarbon dating

The ^{14}C results obtained for the charcoal samples from Level N4 are summarised in Table 3. Finite ages of 36,820 ± 330 ^{14}C yr BP and 38,880 ± 380 ^{14}C yr BP were obtained for samples PVF29373 and PVF29374, respectively. Following calibration (OxCal 4.4, IntCal20), these ages equate to 95.4% C.I. probability ranges of 42,115 to 41,227 calr BP for PVF29373 and 42,945 to 42,295 cal BP for PVF29374.

4.2.3. AAR dating

The concentrations and D/L values of aspartic acid, glutamic acid and serine measured in the teeth samples are shown in Table 4, together with the percentage of these amino acids with respect to the total amino acid content of the samples. Sample LEB-17674 is not considered reliable due to the significant difference between its D/L Asp and D/L Ser values with respect to other samples from the site. The AAR results for the remaining samples indicate that they may have been subjected to anthropogenic heating, as they show a similar pattern to that of heated ostrich eggshells (Brooks et al., 1991; Crisp, 2013) and burned mollusc shells (Ortiz et al., 2020), i.e., the D/L Asp values and % Glx and %Ala were greater than, and %

Asx and %Ser were lower than, the average of archaeological samples with the same age. Indeed, these samples were collected from beds that preserve ash and charcoal evidence for hearth fires. Given that these samples were seemingly subjected to anthropogenic heating, it has not been possible to derive calibrated AAR age ranges using the D/L ratios shown in Table 4.

4.3. Pollen results

The vegetation cover identified from sample C8 is dominated by *Pinus* with low arboreal cover (10.5%), accompanied only by *Juniperus* and *Betula*. *Poaceae* (41.5%) and *Compositae* (25%) comprise the characteristic herbaceous taxa in the open landscape. These preliminary palynological results show that the lower layers of Level 4 correspond to a relatively cold climate, with some degree of humidity. Unfortunately, samples A14, A15, A16, C9 and C10 were sterile and contained no pollen.

4.4. Fauna

4.4.1. Small-mammal assemblage

The small mammal assemblage of the studied samples consists of over 900 remains, 180 (20%) of which were identified taxonomically (80 at species level), yielding an MNI of 32 individuals from 11 taxa (Table 5).

Bone breakage affected 83% of the postcranial elements, with the only complete bones corresponding to phalanxes (7%), metapodials (4%), tarsals (3%) and caudal vertebrae (3%). The long bones show a high level of breakage (100%), while mandibles and maxillae are also affected by an extreme (98%) degree of breakage.

Digestion features (Fig. 4. 1a–e) are observed in 59% of the arvicoline molars and 73.5% of the rodent incisors. In both cases, evidence of digestion reaches extreme levels, indicating that the small-mammal assemblage from Prado Vargas Level 4 was accumulated as a result of predation.

Together, the digestion and breakage levels suggest a Category 4–5 predator. The breakage patterns observed on long bones permit discrimination between avian and mammalian predators according to data published by Andrews (1990), and suggest a mammal carnivore was the main agent responsible for the concentration of small mammal remains in Level 4. The observation of a coprolite matrix adhered to some small mammal bones is also a typical feature of microvertebrate assemblages generated by mammalian predators according to Arriaza et al. (2017) and Domínguez-García et al. (2019).

On the basis of the ecological preferences of the small mammals and their relative abundance (Table 5), we can infer that the landscape around the Prado Vargas site during the formation of Level 4 was mainly wet and dry meadows, with sparse forest cover and abundant rocky zones.

The bioclimatic model results show that when Level 4 formed, the climate at the cave locality was slightly colder than at present (MAT: 9 ± 3.6 °C; Δ: 2 °C), especially in winter (MTC: 3.7 ± 5.8 °C; Δ: 3.7 °C).

4.4.2. Macrofauna

We were able to classify 190 of the 1156 analysed remains (12.1%) taxonomically (Fig. 5), while the rest were classified by size categories due to their heavy fragmentation. The most abundant identified fossils were from *Cervus elaphus* (113), followed by *Capra pyrenaica* (19) and *Equus ferus* (14) (Fig. 6). An NMI of 22 individuals of several ages was documented, most of which were adults.

Calculation of the Isu (anatomical survival index) (Brain, 1969) shows biased skeletal representation in all sizes of the analysed assemblage, indicating systematic selection of anatomical parts with high nutritional and marrow properties. The sample is characterized by the presence of the appendicular skeleton (stylopods, zeugopods and metapods) (Table 6). There are very few remains of the axial skeleton, and these are most abundant in the small size category (20–100 kg).

The cranial skeleton, represented particularly by mandible items, is documented in all weight categories, especially in the medium sizes. Diaphyses were the most abundant long bones (81.9%), followed by metaphyses (14.7%) and epiphyses (3.2%).

Marrow extraction is observed in all size categories and all predominant skeletal elements. Impact features are primarily located on the diaphysis, in the most brittle part of the bone (Olsen and Shipman, 1988). Systematic positioning of some percussive impacts on specific skeletal zones and parts is detected. We found that all impacts on metacarpals were on the ventral face, while on the humerus, the impact are on the dorsal and exterior face. The relatively high presence of mixed angles and bones with evidence of cremation suggests that the bones may have been heated prior to fracturing to facilitate marrow extraction.

A total of 5187 fracture surfaces were analysed. Oblique angles (80.7%), curved lines (44.6%) and smooth surfaces (96.7%) are all found. These percentages were similar in all analysed size categories. We identified 136 notches (Fig. 5), 35 percussion scars, 75 percussion cones and two cases of peeling. In addition, notches are found alongside scars in six cases. A notable 8.6% of notches were opposite and 73.0% were isolated. Their location on the bone surface shows a clear trend, with 95.8% on the diaphysis, primarily on the external and internal faces.

We located 294 cut marks, with 18.7% of bones exhibiting this modification (Fig. 5), mainly on small-size long bones. The most common marks are incisions (89%), both oblique and transversal to the bone axis. The position of the cut marks on skeletal elements is indicative of the animal consumption sequence, including evidence of defleshing on large muscle mass in the form of long incisions (NR = 288) and periosteum scraping (NR = 5). Most cut marks were located on the long bone diaphyses (95.9%) (Fig. 6).

Heat-induced alteration was also present in 5% of the remains from Level 4 (NR = 79), with State 4 being the most abundant (greyish colouring).

Carnivores produce bite marks and fractures, mainly on the appendicular skeleton. A total of 133 bone remains (8.4%) were found with modifications made by carnivores (Fig. 6). They included pits and grooves (NR = 111), crenulated edges (NR = 7), diaphyseal cylinders (NR = 2) (Fig. 5), digestion (NR = 6) and pitting (NR = 7). The dimensions of the bite marks on hard cortical material ranged between 0.2 and 7.4 mm long and 0.1 and 3.8 mm

Table 3
AMS ^{14}C dating results for isolated charcoal samples obtained from level N4. ^{14}C analyses were undertaken at BETA Analytic Inc. Laboratories. Calibration has been undertaken using OxCal 4.4 and IntCal20.

Level	Sample ID	Lab ID	Material	Pre-treatment	δ^{13}C	Uncalibrated ^{14}C age (^{14}C yr BP ± 1σ)	Calibrated ^{14}C age (95% C.I. cal. BP ranges)
N4	PVF29373	Beta-548,572	Isolated charcoal	Acid-base-acid	−25.8‰	36,830 ± 330	42,115 − 41,227
N4	PVF29374	Beta - 548,573	Isolated charcoal	Acid-base-acid	−25.6‰	38,890 ± 380	42,945 − 42,295

Table 4
Concentration (pmol/mg), D/L values and percentage of aspartic acid, glutamic acid and serine in the tooth collagen samples from Prado Vargas Level 4.

Level	Sample	Genus	D Asp (pmol/mg)	L Asp (pmol/mg)	D/L Asp	D Glu (pmol/mg)	L Glu (pmol/mg)	D/L Glu	D Ser (pmol/mg)	L Ser (pmol/mg)	D/L Ser	% Ala	% Asp	% Glu	% Ser
N4	**17,528**	*Equus*	8278.4	60945.6	0.136	6757.2	119935.6	0.056	1542.3	45178.6	0.034	34.3	10.0	18.3	6.8
	17,529	*Bovidae*	590.3	4091.7	0.144	445.8	6964.3	0.064	113.2	2599.1	0.044	19.9	7.3	11.6	4.2
	17,530	*Equus*	892.7	4695.5	0.19	900	9322.2	0.097	55.5	2502.8	0.022	21.4	6.4	11.8	2.9
	17,531	*Ursus*	1875.5	17,276	0.109	1220.9	29324.4	0.042	129.5	12002.7	0.011	19.0	6.9	10.9	4.3
	17,532	*Equus*	1812.4	15358.6	0.118	1240.8	27298.8	0.045	322.7	11444.2	0.028	19.4	6.7	11.1	4.6
	17,533	*Arctiodactyla*	1782.2	15177.6	0.117	1163.3	26166.5	0.044	33.3	10004.1	0.003	19.9	6.9	11.2	4.1
	17,534	*Cervus*	1955.0	16438.5	0.119	1442.9	27958.9	0.052	306.1	10177.4	0.030	20.5	7.1	11.3	4.0
	17,535	*Arctiodactyla*	1933.0	19256.9	0.100	1340.9	32,490	0.041	311.1	13067.8	0.024	19.9	7.0	11.2	4.4
	17,536	*Ursus*	2359.6	22693.6	0.104	1735.1	44475.9	0.039	495.8	20,842	0.024	5.9	13.2	24.3	11.2
	17,537	*Cervus*	2536.9	22,999	0.11	1698.2	39045.2	0.043	465.6	15070.7	0.031	31.0	10.6	16.9	6.5
	17,538	*Equus*	3632.9	31229.5	0.116	2410.7	55574.1	0.043	716.2	23393.3	0.031	13.3	12.7	21.1	8.8
	17,540	*Meles*	1750.8	14834.6	0.118	913.7	24984.9	0.037	311.6	10887.5	0.029	18.3	6.9	10.8	4.7
	17,671	*Ursus*	339.5	3405.6	0.100	212.1	7853.5	0.027	94.3	3457.8	0.027	21.4	13.2	24.3	11.2
	17,672	*Ursus*	4545.2	42832.9	0.106	2779.1	90795.1	0.031	936.8	39618.8	0.024	5.9	13.7	24.8	11.7
	17,673	*Ursus*	122.3	1009.9	0.121	65.1	2319.9	0.028	30.1	1072.4	0.028	20.5	12.7	23.8	10.7
	17,674	*Ursus*	547.5	2465.6	0.222	391.4	5802.7	0.067	402.6	2230.1	0.181	31.0	13.2	24.3	11.2
	17,675	*Ursus*	19373.5	173580.5	0.112	16024.7	102453.8	0.156	4135	122222.1	0.034	13.3	24.3	13.2	13.5
	17,676	*Ursus*	17384.4	155314.5	0.112	9731.7	117,471	0.083	2771.1	114448.9	0.024	34.3	24.8	13.7	14.0
	17,677	*Ursus*	3755.7	28,728	0.131	2308.3	63840.3	0.036	856	25687.4	0.033	19.9	12.9	24.8	11.5
	17,678	*Ursus*	500.5	6105.1	0.082	295.3	13287.9	0.022	116.4	5766.3	0.02	18.3	13.4	25.3	12.0
	17,679	*Ursus*	1374.7	9331.7	0.147	853.1	20,078	0.042	420.4	8027.1	0.052	21.4	12.4	24.3	11.0

Table 5
Small-mammals assemblage from level 4 of Prado Vargas. Number of identified specimens (NISP); minimum number of individuals (MNI); most common element per species (Element); relative abundance based on MNI (%MNI); distribution by habitat type: open humid (OH); open dry (OD); rocky areas (Ro); open woodland (OW).

	NISP	MNI	Element	%MNI	OH	OD	Ro	OW
Arvicola amphibius	11	2	right M_1	6.25	1			
Microtus arvalis	12	8	left M^1	25.00		0.75		0.25
Microtus gr. *agrestis*	10	6	left M^1	18.75	0.5			0.5
Microtus cf. *lusitanicus*	2	1	right M_1	3.13	0.5			0.5
Chionomys nivalis	4	3	left M_1	9.38			1	
Pliomys coronensis	19	5	right M_1	15.63			1	
Apodemus cf. *sylvaticus*	12	3	right M^2	9.38				1
Eliomys quercinus	2	1	left M^1	3.13			0.25	0.75
Sorex coronatus-araneus	7	1	right M_1–M_2	3.13	0.75			0.25
Talpa sp.	1	1	left lower M	3.13	0.75			0.25
Lepus sp.	6	1	humerus	3.13		1		
Arvicolinae	47		molars					
Rodentia	49		incisors					
	180	32		100.00				

wide. Measurements on soft cortical bone remains ranged between 0.4 and 5.8 mm long and 0.5 and 2.6 mm wide. On the basis of measurements published by authors such as Andrews and Jalvo (1997), Selvaggio and Wilder (2001); Domínguez-Rodrigo and Piqueras (2003), Yravedra (2004), DelaneyRivera et al. (2009) and Arilla et al. (2014), these data could match a wide range of predators. However, the range of bite mark dimensions seems to match the carnivores recorded in the cave (*Ursus spelaeus*, *Canis lupus* and *Meles meles*), although other predators cannot be ruled out. Perhaps the low incidence of carnivores is due to secondary access to faunal remains. The presence of modifications produced by carnivores lead us to discard them as the main accumulative agent and as an element of significant distortion of the original assemblage.

The fossil-genetic alterations, include trampling (77.45%), cracks (73.17%), polishing (80.17%) and manganese coatings (89.03%).

4.5. Lithic assemblage

4.5.1. Raw materials

Several types of raw material were documented. Flint accounting for 91.9% of the total recovered material. This material was collected from the cave surroundings and also included blanks from inside the cave itself. The raw materials were collected as pebbles and nodules sometimes. From primary outcrops and secondary deposits. Analysis proved the local capture of this material by the Neanderthal occupants of Prado Vargas (Navazo et al., 2005; Vallejo et al., 2017).

4.5.2. Technology

All structural categories are represented in the Level 4 lithic assemblage. Forty-six of the 68 recovered cores are on pebble (BN1Ge) and the remaining 22 were on flake (BN2Ge). Thirty-eight were intact (21 BN1Ge and 17 BN2Ge) and the rest were fractured. All but two were Cretaceous flint, with the exceptions being lutite (BN2Ge) and a piece of quartz (BN1Ge); the only specimen of this material recovered so far from N4. The 38 intact specimens included two unifaces, both made from Cretaceous flint. One of them was centripetal or unifacial secant (Carmignani et al., 2017), on flake and exhausted, and the second was bipolar opposite (BN1Ge), of poor quality and therefore may have been discarded. Eighteen of the 36 bifaces were BN2Ge and 18 were BN1Ge. Exploitation was predominantly on the large face (Carmignani et al., 2017) (Table 2), with peripheral (52%) and polar exploitation, depending on the organisation and location of the striking platform. Peripheral exploitation was on secant (65%) and parallel (35%) planes, depending on the removal angle.

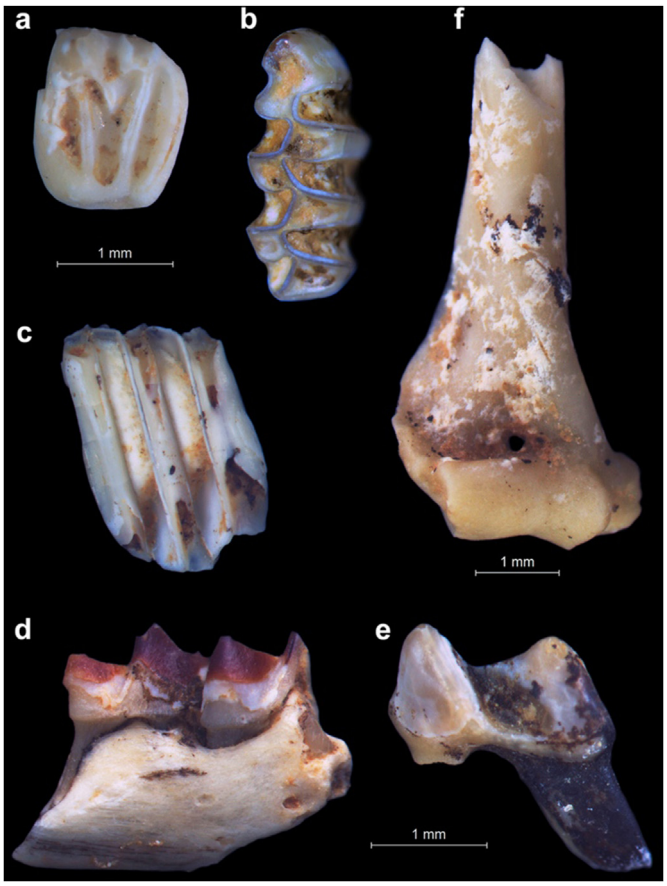

Fig. 4. Predation features shown by micromammal remains from level 4 of Prado Vargas. Right M^2 of *Eliomys quercinus* with heavy digestion in occlusal view (a). Left M_1 of *Microtus* gr. *agrestis* with moderate digestion in occlusal view (b). Left M_2 of *Microtus* gr. *agrestis* with heavy digestion in labial view (c). Right mandible fragment with M_1–M_2 series of *Sorex* gr. *coronatus–araneus* with heavy digestion (d). Left lower molar of *Talpa* sp. with heavy digestion (e). Right humerus of a vole with adhered coprolite matrix (f).

On the basis of core symmetry and hierarchy of the flaking faces (Vaquero et al., 2008), the exploitation systems were found to be predominantly asymmetrical hierarchical, followed by symmetrical non-hierarchical, symmetrical hierarchical and finally asymmetrical non-hierarchical. There was also one bipolar opposed core, one unipolar opposed core, one multifacial core and six three-facial cores. These items are noteworthy as they were probably bifacial in origin (D1) and then fractured, which generated a third face that was exploited. Thirty-eight of the 68 cores bear evidence of fire. The most noteworthy aspect of these items is that 21 were recycled (denticulates, sidescrapers, points and one endscraper).

We found 587 flakes, 188 of which were flake fragments or fractured flakes. The flakes were predominantly flint (95%), followed by quartzite and lutite. The defining features of this category were determined by analysing their dorsal and ventral faces. Butts were predominantly non-cortical (75%), followed by cortical (2%), with the remainder being nco (co) and co (nco). The most represented butt surface was platform (66%), followed by linear (14%) and pointed (5%). The rest could not be distinguished due to proximal fractures. The dorsal faces of the flakes were primarily non-cortical (88%), cortical (1%) and, in a few cases, cortex. Shaping was primarily unifaceted (58% of all items), followed by bifaceted (11%), multifaceted (4%) and non-faceted (1.3%). The typometry of non-retouched products was predominantly micro (<4 cm) and small (>4 cm < 6 cm) sizes, including broad and quadrangular flakes. These items matched the production pattern found on the cores from this site.

The discoid and Levallois exploitation systems generated (i) flakes with cortex removal or entame flakes, and others with residual cortex; (ii) natural backed blades and flakes with markedly centripetal prior removals on the dorsal face; (iii) many débordante and overshot flakes, and; (iv) several pseudo-Levallois points. Kombewa flakes were also found. Some thicker flakes (probably the result of the Quina system) and general quadrangular butts were found, as as well as a few flake blades and bladelets. Several Siret fractures are observed, some with double patina.

With regards to configuration, 98 tools are classified as retouched; 96% of which are flint and the other 4% quartzite. The retouched blade butts are predominantly non-cortical (81%), with very few cases of cortical (2%) or retouched. Most are platform butts, and 4% are linear. In terms of shaping, 69% of the retouched flake butts are unifaceted and 21% bifaceted, followed by multifaceted. Most dorsal faces are non-cortical, with only two items showing a completely cortical dorsal face. The size of most retouched items is somewhat larger than the unretouched flakes, mostly micro- and small-sized. The majority (62%) of retouches are classed as the simple mode (62%), followed to a much lesser extent by abrupt (18%), semi-abrupt (13.5%), stepped (4.2%), and flat (2.3%) modes. The width of the retouch is marginal in most cases, with 50% displaying a continuous line, along with denticulates (33%) and notched (17%). Orientation is direct (67%) and inverse (33%), and the lines of the blade is convex and sinuous (both 35%), followed by straight and concave. The location of these retouches is primarily on both sides, followed by modifications to the blade by retouching on the distal transversal face.

On the basis of the detected exploitation systems, the retouched items are generally configured on thick Levallois and a few Kombewa flakes. The most representative type is the sidescraper (just over 37%), followed by denticulates (36%), notches (15%) (Fig. 7 F–K), and, with much less frequency, points and scrapers.

Lithic manufacture inside the cave was aimed at producing small butts, which in most cases are functionalised on their unworked edges. Retouched products seem to have also been manufactured inside the cave, considering the large number of bone retouchers found here. In conjunction with the recurrence of simple retouch on sidescrapers, and the marginal presence of Quina or semi-Quina retouch, this evidence shows that the bone fragments were used to modify flake blades by means of simple retouch.

4.5.3. Traceology

Comparison of experiments conducted on modern materials confirm similar usage of the recovered lithic tools from Level 4; although the exact production and usage traits of the total assemblage could not be ascertained due to the small sample size involved in the traceology study. From the preliminary study of ten Cretaceous flint tools from the Prado Vargas site, two were found to have been used for hide scraping (Fig. 8), two for wood processing (8B), and four for meat processing (Fig. 8C), (Santamaría et al., 2016).

4.6. Bone retouchers

The bone fragments recovered from Level 4 measured between 6.7 mm and 193 mm. The smallest fragment used as a retoucher measured 21.1 mm, while the largest was 133.8 mm. The size interval with the greatest concentration of retouchers was the 60–80 mm range. Anatomical identification of the bone blanks is not always easy, but it was possible to identify 33 fragments, all confirmed as limb bones. The majority of these fragments were

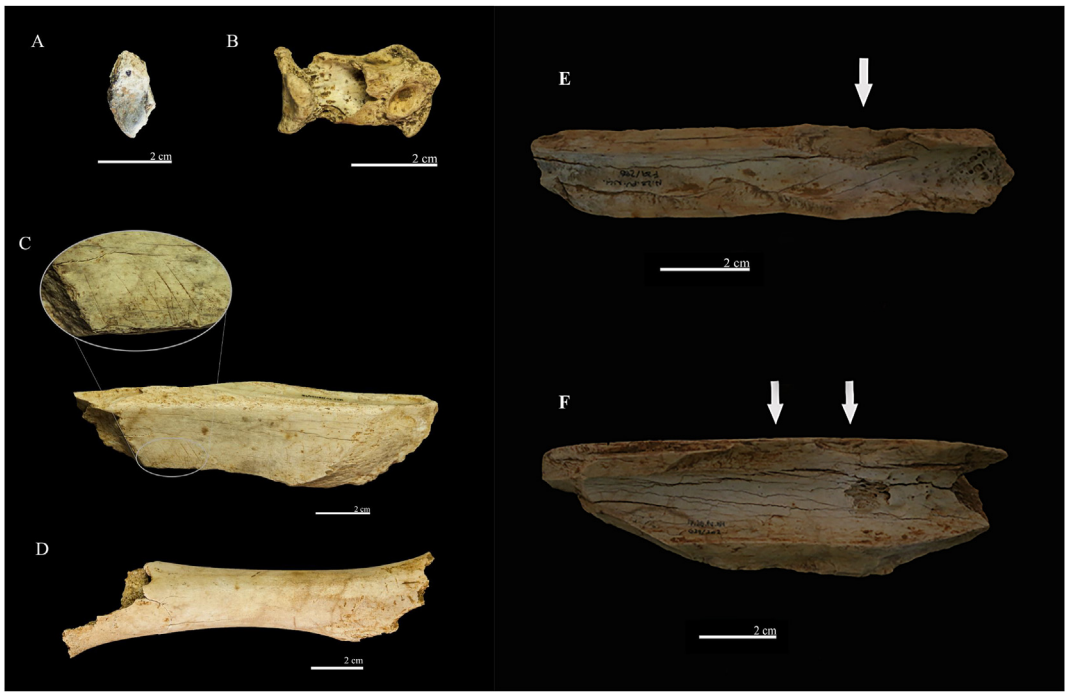

Fig. 5. Modifications located on Level 4 of Prado Vargas. A: Thermally altered bone. B: Phalanx of *Cervus elaphus* digested by a carnivore. C: Large bovid tibia with cut marks. D: Long bone of small size with carnivore pits and diaphyseal cylinder morphology. E: Isolated percussion notch. F: Consecutive percussion notches.

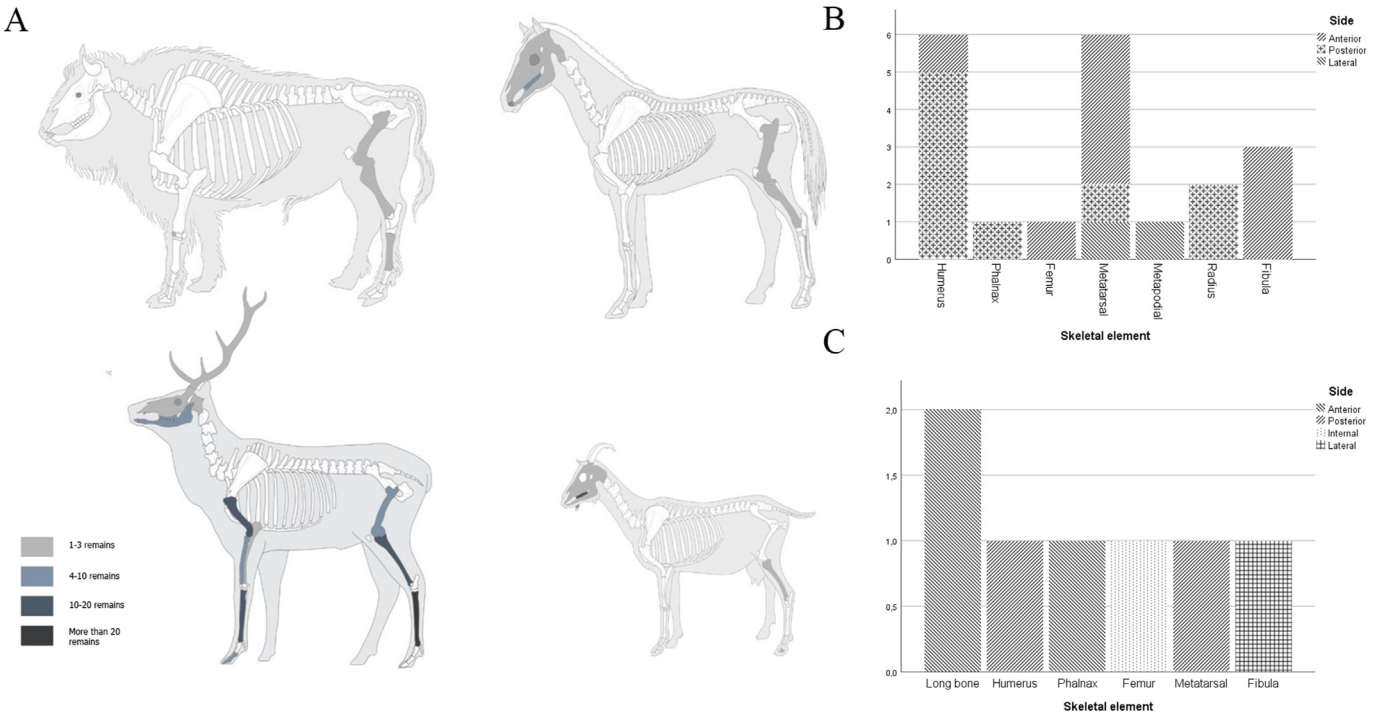

Fig. 6. Faunal assemblage. A: Most representative skeletal elements. B: Cut marks and its relation with the skeletal elements. C: Carnivore pits and scores and its relation with the skeletal elements.

from the humerus (16.1%), followed by tibia, femur and metatarsus fragments (7.3%). When extrapolating this information to the entire archaeological level, it appears that the humerus was one of the most common remains used for retouchers; nevertheless, other common bones, such as tibia and metatarsus, were used in the same way as the more commonly occurring bones, such as femurs (Fig. 9).

In the analysed sample, seven of 68 items showed more than

Table 6
Number of remains according to taxon and anatomical element (NISP). Minimun Number of Elements (MNE). Minimun Number of Individuals (MNI). General utility indices based on Emerson (1993) data and their correlation with ISu% (Anatomical survival index) according to weight sizes.

Taxa					Anatomical elements			
		NISP	MNE	MNI		NISP		NISP
Talla grande (1000-300 kg)	*Ursus spelaeus*	7	7		Phalnax	5	Humerus	72
	Equus ferus	14	13	3	Residual metapodial	1	Scapula	6
	Bos-Bison	6	5	1	Metapodial	27	Coxal	2
Talla media (300-100 kg)	*Cervus elaphus*	113	36	3	Metatarsal	44	Rib	34
Talla pequeña (100-20 kg)	Caprinae	7	2		Metacarpal	36	Vertebra	12
	Capra pyrenaica	19	16	3	Carpal/Tarsal	3	Mandible	18
	Rupicapra pyrenaica	11	9	3	Sesamoid	1	Maxilar	4
	Sus scrofa	1	1	1	Tibia	86	Teeth	110
	Meles meles	3	1	1	Femur	42	Cranium	24
	Canis lupus	7	3	3	Ulna	9	Antler	3
Talla muy pequeña (>20 kg)	*Leporidae*	2	2	2	Radius	56		

	General utility	Food utility	Fat	Marrow volume	%Isu large size	%Isu medium size	%Isu small size
Mandible	25,5	10,4	–	–	25	66,67	42,86
Vertebra	47,4	61,7	100	0	0,96	1,28	1,1
Rib	62,3	71,3	93	0	0	1,28	2,2
Coxal	34,7	39,8	54	3,9	12,5	16,67	14,29
Scapula	25,5	28,4	30,4	40,6	12,5	33,33	14,29
Humerus	27,5	28,4	30,4	79,8	62,5	83,33	42,86
Radius-Ulna	19,1	19,7	22	69,4	37,5	33,3	32,1
Femur	100	100	76,7	93,5	62,5	66,67	57,14
Tibia	57,7	58,1	48,6	100	50	83,33	28,57
Metacarpal	5,4	6	8,4	30,3	25	66,67	7,14
Metatarsal	10,8	15,9	16,1	40,8	0	83,33	0
Phalnax	3,9	8,4	9,2	22,2	0	6,94	1,79
Pearson's r							
General utility					**0,413700148**	**−0,002989**	**0,46179499**
Food utility					**0,284449324**	**−0,137,175**	**0,281448811**
Fat					**−0,047915231**	**−0,409,425**	**0,066780334**
Marrow volume					**0,884303345**	**0,7697769**	**0,831824235**

one active area, with none exceeding two areas. The size of these areas ranged from 2.1 mm long x 2.1 mm wide in the case of PV′17/4/G28.82, to 22.6 mm long x 9.8 mm wide in the case of PV′17/4/G28.82. The actives areas tend to be longer than wider, possibly due to the shape of the fragments. Following the distinction employed by Mallye et al. (2012), the concentrated areas of use comprise 50.6% of the sample, followed by dispersed (25.3%) and superimposed (17.3%) zones. The least represented type was isolated areas (6.6%). Some differences were also observed in the location of active areas. There was a predominance of active areas toward the left of the item (44.9%), followed by those toward the right (30.4%) Consideration of the results of previous experimental research gave us a better idea of the way that these tools were used (Alonso-García, 2020.). Using these empirical datasets, we are able to make a distinction between retouchers that had little use, medium use, and intense use (Mozota, 2012). Items used during a short period showed an average of 25.6 mm of use wear, those with medium use showed an average of 34.1 mm of use wear, while those with intense use showed an average of 18.4 mm of use wear. In all cases, there were more linear impressions than pits.

4.7. Human remains

Prado Vargas 1360 (Fig. 10) is a complete, well-preserved tooth crown with resorbed roots. The crown shows some post-depositional fractures, which affect the enamel and the exposed dentine on the occlusal surface. The distal surface, where most of the enamel is absent, is the most heavily affected section. The crown is worn, showing stage 4 advanced occlusal wear (Molnar, 1971), with dentine exposed on all cusps. The roots show clear evidence of resorption, indicating that the tooth was lost in life due to dental replacement.

The tooth is a deciduous lower left first molar (Ldm_1) with four main cusps, however the occlusal dental degree hinders confirmation of a possible fifth cusp, the hypoconulid. The outline of the crown is rectangular in occlusal view. The interproximal wear facet is present on the mesial face, however it was lost due to post-depositional damage on the distal face. We were able to identify some non-metric traits on the occlusal surface such as a mesially-located anterior fovea, but due to its wear, it was not possible to confirm the presence of an enamel ridge connecting the metaconid and protoconid. The shape of the exposed dentine in this zone seems to be indicative of the existence of a mid-trigonid crest at enamel-dentine junction (EDJ). Nevertheless, confirmation of this non-metric trait will be possible following ongoing analysis of EDJ based on microCT data. Finally, the mesiobuccal part of the crown, the *tuberculum molare*, shows pronounced bulging.

The MD and BL tooth crown dimensions are 8.62 mm and 7.36 mm respectively (see Table 7 for comparative data). Metrically, both the MD and BL dimensions of Prado Vargas 1360 match well with the mean of our Neanderthal comparison sample (MD, n = 9, 8.68 and BL, n = 9, 7.39); but are out of the range of Upper Palaeolithic and Mesolithic Europeans.

5. Discussion

5.1. Stratigraphic, chronological and palaeoenvironmental context of level N4

The Prado Vargas karst infill sequence was primarily formed during a succession of fluvial events involving alternating flows of variable energy. These infilling processes deposited sand and a smaller amount of gravel, and were the result of numerous waterlogging processes caused by overflowing channels, possibly

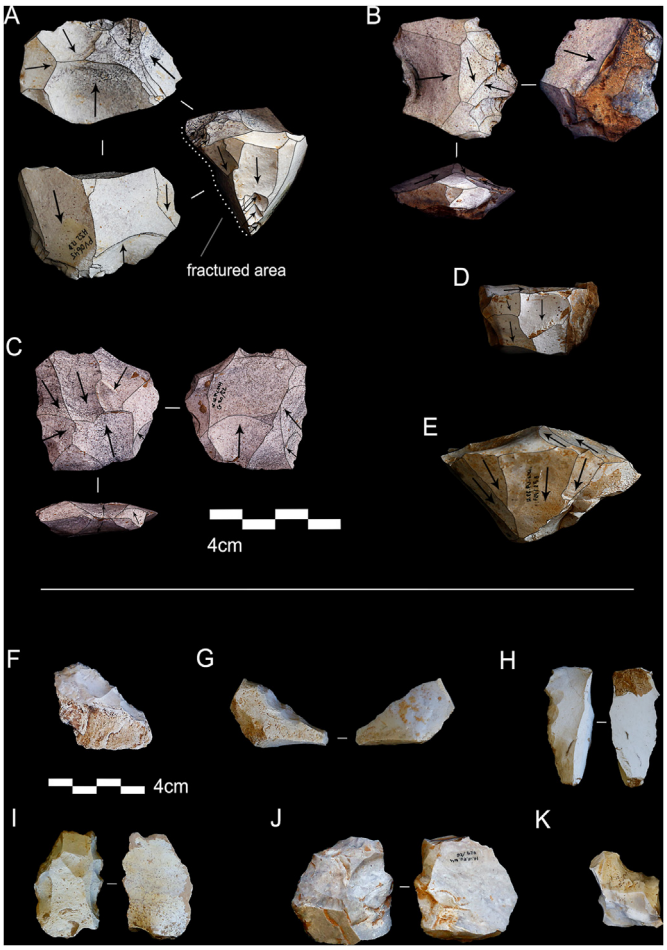

Fig. 7. Lithic assemblages from Level 4. A-E cores (B y C retouched), F– K retouched flakes or fragments.

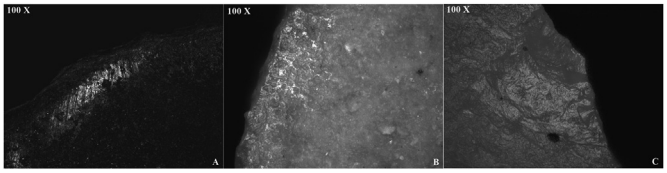

Fig. 8. Selection of flint tools from the sample: A)Tool PV06–N4–H31-105, polish and striations related to hide scraping. B) Tool VA-α1-N4-132, polish and rounding related to wood working. C) Tool PV06– N4-G31-50, polish and scars related to meat processing.

Fig. 9. Bone retouchers from Level 4.

Fig. 10. Different views of PV-1360 tooth: A: Mesial; B: Occlusal; C: distal; D: Buccal; E: radicular.

augmented by dripping from the cave roof. The yellowish sandy fluvial facies suggest an internal source, implying that the sedimentation episodes were linked to moister phases that resulted in reactivation of the karst system and made the cave act as a spring.

The formation of Unit PV4, which contains archaeological Level N4, is mainly associated with decanting processes. To date, it has not been possible to differentiate the discontinuous local stratification planes of the clayey facies in Unit PV4. However, these stratifications do show that the package was deposited over several events, raising the possibility for seasonal occupation of the cave. These events are mainly characterized by clays, but layers of sand and clay with a high gravel content are also present, with spatial differentiation beginning near the western part of the excavation site. The sedimentary characteristics of these PV4 deposits suggest formation by waterlogging processes, which were likely the result of overflowing watercourses running through the cave during wetter periods.

The chronology of Level N4 has been constrained using single-grain OSL and AMS ^{14}C charcoal dating in this study. Unfortunately, it was not possible to derive meaningful AAR age for the latest teeth samples analysed from Level N4 owing to anthropogenic heating effects. The OSL samples from the middle of Level N4 yielded 2σ age ranges of 54.7–41.9 ka (PRA19-1) and 52.6–39.8 ka (PRA19-2), consistent with the previously obtained AAR age of 46.4 ka for a horse tooth from Level N4 (Navazo et al., 2005). The corresponding 95.4% C.I. calibrated ^{14}C age ranges for the basal layers of Level N4 are 42,115–41,227 (Beta-548,572) and 42,945–42,295 (Beta–548,573) cal BP, which overlap with the lower 2σ boundary ranges for both OSL samples, although the ^{14}C ages are systematically younger by several millennia.

Given the close agreement between the mean OSL ages (46.2 ± 3.2 and 48.3 ± 3.2 ka at 1σ) and the mean AAR age for Level N4 (46.4 ka), the systematic ^{14}C age offset could be indicative of minor problems related to incomplete removal of organic contaminants (e.g., Higham, 2011; Becerra-Valdivia et al., 2020). The standard acid-base-acid ^{14}C pre-treatment procedures employed in this study are typically sufficient to eliminate carbonates and humic contaminants in the case of relatively young charcoal samples (e.g., <20 ka cal BP). However, dating comparisons undertaken at several prominent European Palaeolithic sites (e.g., Brock and Higham, 2009; Douka et al., 2010; Wood et al., 2012; 2013; Higham et al., 2009; 2014; Devièse et al., 2017) have shown that older charcoal samples approaching the upper dating limits of the ^{14}C method can underestimate "true" ages by several millennia if more rigorous preparation procedures designed to remove exogenous carbon are

Table 7
Metric dimensions of Prado Vargas 1360 compared to other Neanderthal and *Homo sapiens* specimens (Arnold et al., 2016(1), Hershkovitz et al., 2016(2); Faerman et al., 1994(4); Trinkaus and Walker, 2017(5); Mizoguchi, 2002(3)). * Data calculated in this study from MD and BL data available in the references cited. Crown area = MD*BL; Crown index= (BL*100)/MD.

dm_1	MD (mm)	BL (mm)	Crown area (mm^2)*	Crown index*
Prado Vargas 1360	8.62	7.36	63.44	85.38
Neanderthals (n = 9)* (1,2,3)	8.68	7.39	64.14	85.13
European Upper Paleolithic (3)	9.03	7.7	69.53	85.27
European Mesolithic (3)	8.1	7.2	58.32	88.8

not employed (e.g. acid-base-wet oxidation-stepped combustion – ABOx-SC; Bird et al., 1999, 2014). Without stringent ABOx-SC pre-treatment of the Level N4 charcoal samples and further examination of the effects of progressive contaminant removal, we cannot rule out the possibility of minor ^{14}C age underestimations in the present study.

An alternative explanation for the minor age offset between the ^{14}C and OSL samples could be that the latter were affected by protracted sediment residence times within the cave environment prior to their final deposition. However, this explanation seems less likely, as the single-grain D_e analysis and age models employed in this study were chosen to provide direct constraints on such depositional complications as part of the final OSL age calculations (see further discussions in Demuro et al., 2019b). Irrespective of the causes of the minor age offset, it is worth emphasising that the OSL and ^{14}C ages for Level 4 are statistically indistinguishable at the 95.4% C.I. As such, both datasets can reasonably be combined for chronological assessment of Level N4, yielding a most probable age range of between 54.7 and 39.8 ka BP.

The fossildiagenetic alterations observed on the archaeological material indicate water alterations in the cave environment. Some of the lithic material has a shiny surface, characteristic of immersion in waterlogged areas, while the edges and the materials in general, appear to be in a relatively fresh state. Concretions and remains of manganese oxide were also observed on the lithic and faunal materials, providing evidence for the presence of moisture and the existence of puddles, or water flow of greater or lesser intensity. The presence of water is corroborated by bones with a considerable amount of polishing and rounding, which affects both the medullary and cortical sides. Other alterations to the material, such as abrasion, may have also depended on the sedimentary matrix (Shipman, 1981; Bromage, 1984). Trampling or water flow may be the cause of the short movement of the remains. Finally, the presence of vermiculation marks on some of the remains indicates the existence of light in the cave, and corroborates the presence of more or less permanent moisture during the formation of Level N4. The scarcity of weathering could be related to relatively rapid rate of sedimentation and/or to constant humidity and temperature conditions inside the cave; which would have prevented more abundant or more advanced stages of diagenetic alteration.

During the formation of Level 4, the landscape was composed of open herbaceous spaces dotted with a few coppices of pine, along with the localised presence of *Juniperus* and *Betula*, suggesting cold climatic conditions with a degree of humidity. Climatic crises during MIS3 are considered to have been an active agent in Neanderthal demise in the Iberian Peninsula, causing significant drops in temperatures and changes to arid paleoenvironmental conditions (Jiménez-Espejo et al., 2007; d'Errico and Sanchez Goñi, 2003; Madrid Sepulchre et al., 2007). Recent $\delta^{13}C$ stable isotope analysis on ungulate bones from the north face of the Cantabrian region, just to the north of Prado Vargas site, suggests a shift in regional climate before the conclusion of Mousterian, characterized by a change in the dominant vegetation to more open landscapes (Jones et al., 2018).

These climatic inferences are confirmed by t he pollen study, as well as by macro- and micro-fauna indicator species at Prado Vargas. Large fauna that are characteristic of open spaces (Equus ferus and Bos/Bison), more closed spaces (Sus scrofa, and Canis lupus), and taxa that inhabited both types of environments (*Cervus elaphus* and *Oryctolagus* sp.) are well represented in the fossil assemblage. MIS 3 is a period characterized by relatively rapid changes, from intense cold to temperate conditions. Episodes of extreme cold are revealed by nearby fossil assemblages of cold-adapted large-mammals, such as woolly mammoth (*Mammuthus primigenius*) (Altuna and Mariezkurrena, 2000; Álvarez-Lao, 2014), woolly rhinoceros (*Coelodonta antiquitatis*) (Castaños, 1996; Álvarez-Lao, 2014) and reindeer (*Rangifer tarandus*) (Altuna, 1971a, 1980; Altuna and Mariezkurrena, 2000; Castaños, 2005). However, these cold-adapted taxa occurrence with other species such as reed deer (*Cervus elaphus*), roe deer (*Capreolus capreolus*), ibex (*Capra pyrenaica*), chamois (*Rupicapra pyrenaica*), horse (*Equus ferus*) and aurochs/bison (Bovini or *Bos/Bison)* (Álvarez-Lao, 2014). At Prado Vargas, the taxonomic profile may reflect cold episodes, but these do not appear to have been as intense as those recorded at La Güelga, Covalejos, El Castillo, El Pendo, Cueva Morin or Arrillor (Altuna, 1971b, 1973; Fuentes Vidarte, 1980; Pike-Tay et al., 1999; Castaños, 2005; Menéndez et al., 2018; Iriarte-Chapiusso et al., 2019; Luret et al., 2020).

The small mammal assemblages suggest a combination of forest steppes with temperate elements, and also grassland and scrubland. The spread of some glaciers in the Cantabrian Mountain Range peaked 45 ± 3 ka ago (Jiménez-Sánchez et al., 2013), which would be consistent with our interpretation that ambient temperatures associated with Level 4 were lower than those currently experienced in the region.

5.2. Neanderthal subsistence strategies and cultural traditions

The Level 4 archaeological record shows that Neanderthals travelled through a range of local environments, and that when they obtained prey, particularly small and mediumsized adult ungulates, they selected anatomical parts with high nutritional and marrow content and took them into the cave. The heavily fragmented bones show that the prey were processed in the cave with activities such as defleshing or bone fracturing to gain access to the marrow, with intensive use made of the animal carcasses. Only a minority of fossil remains exhibit irregular edges, indicating fragmentation in a dry state or as a result of other processes such as trampling or sedimentary pressure.

During the various occupation episodes of Level N4, flint was gathered from areas near to the cave, seemingly a general trend with Neanderthal groups (Navazo, 2008; Navazo and Carbonell, 2014; Moncel et al., 2019), while little allochthonous material (quartzite and lutite) was brought into the cave in the form of end products. Over 90% of the assemblage was made from similar-quality flint. Neither the quality nor the shape of the blocks or nodules therefore seem to have influenced the chosen debitage system. More elaborate toolkits made from allochthonous raw

materials have been found at sites such as Axlor (Ríos, 2005) and Sclayn Cave, Aquitaine (Otte, 1998), where they were brought into the caves in the form of configured tools. This is the case for the flint sidescrapers from Axlor, Teixoneres (Sánchez-Hernández et al., 2014), Abric del Pastor (Machado et al., 2013) and also Level 2 at Jarama VI (Navazo et al., 2020). These attributes may reflect the fact that, while on the move, the Neanderthal groups carried a basic toolkit which they could use and leave behind at these sites.

The exploitation systems fit perfectly with what can be defined as hierarchical discoid knapping, an intermediate method between discoid and Levallois debitage. These types of systems produce variable morphologies as they make use of the recurrence principle on the blanks. The end results are morphologically close to Levallois and laminar methods.

In recent years, it has been proven that there is a relationship between mousterian sites with discoid technology and local raw materials, and cyclical and seasonal movements such as Grote di Fumane (Delpiano 2018); Sclandina cave (Moncel, 1998); Champ Grand (Slimak, 1999); Combe Grenal (Faivre et al., 2014), archaeological sites of Cantabria (Carrión et al., 2008), such as El Castillo (Sánchez- Fernández and Bernaldo de Quirós, 2008) and Cueva Morin (Maíllo, 2007). Similarly, we think that the evidence from Level N4 of Prado Vargas indicates prolonged and residential occupation, and possibly seasonal occupation by Neanderthals.

This region contains abundant flint resources, andthe same types are regularly gathered from different places by the Prado Vargas inhabitants. From this use of local raw material we can infer limited mobility during the Level 4 occupations. In addition, discoid technology is associated with low mobility at other sites such as Grotte du Noisetier (Mourre and Thiébaut 2008). Regarding other resources, it has recently been in recent times how Neanderthal mothers are associated with places that have abundant local resources for rearing infants (Nava et al., 2020).

The Prado Vargas Neanderthal groups employed a recycling economy. They recycled bone fragments (primarily limb bones, along with humerus, femurs and metatarsus) obtained from their food sources by introducing them into the technological sphere, and turning them into retouchers. The available evidence suggests that the less common bone fragments were chosen as retouchers. Despite the high percentage of flat bones (8.6%) and teeth (4.2%) recovered from the site, these items were not selected for use, as documented at other archaeological sites such as La Quina (Verna and d'Errico, 2010) and Les Pradelles (Costamagno et al., 2017). In most cases, the criteria for selecting bone fragments seems to have been their size and their freshness. The most likely explanation is that the bones used as retouchers were collected and broken immediately after the flesh was removed. Seven of the bone retouchers showed more than one area of use, suggesting that they may have been used more than once, possibly during the same knapping event or perhaps at different times. The differences in the location of the active areas (right, left or centred) may reflect the use of retouchers by different-handed individuals as as noted in the studies of Semenov, 1981; Rigaud, 1997; Uomini et al., 2011 and Mozota Holgueras, M., 2012 said in their studies. The handedness of individual in the past has been shown in the production of flakes (Dominguez-Ballesteros and Arrizabalaga 2015a; 2015b; Bargalló et al., 2016) and other later elements, such as sharpened hand axes (Dominguez-Ballesteros and Arrizabalaga 2014) and even in the grooves on people's teeth (Bermúdez de Castro et al., 1988; Frayer et al., 2016).

The high percentage of bone retouchers and the limited number of retouched flakes found in Level 4 could be due to at least two reasons. First, bone retouchers may also have been used to exploit cores, since many are micro-sized and the removal of the final flakes would have been more efficient for continuing processing activities. Second, the inhabitants of Prado Vargas retouched the flakes *in situ* and abandoned them outside the cave (Costamagno et al., 2018).

In addition, the cores were recycle in two ways: 1. Originally bifacial volumes with orthogonal and secant removals were fractured to produce a third face, which was then exploited (Fig. 7A) 2. Exhausted cores were recycled into retouched tools (Fig. 7 BC). Some flakes were also found with scars on the ventral face, possibly flakes that had been recycled into cores, or items that were thinned for some reason. The removal of microproducts from flake cores leaves characteristic negatives in the form of Clactonian notches, a process studied elsewhere for the ramification of the chaîne opératoire in the discoid exploitation system (Bourguignon et al., 2004). This intense use of raw materials resulted in a variety of core exploitation and handling attributes found not only at Prado Vargas but also other sites such as Abric Romaní (Capellades, Barcelona) (Vaquero, 2008.), Bolomor (Cuartero 2007) and Axlor Biscay) (Ríos et al., 2015), as well as at French sites including Champs-de- Bossuet, Pech de l'Azé and Combe Grenal (Thiébaut, 2013). The intense recycling of cores has been interpreted at sites such as Abric Romaní, as evidence of the use of raw material at different moments in time (palimpsests). The Prado Vargas technology is characterized by the discoid knnaping system. Discoid technocomplexes are generally conceived as a technological response by human groups associated with cyclic and seasonal mobility and strictly adapted to local territory (Delagnes and Rendu, 2011; Turq et al., 2017; Martellota et al., 2020)

In contrast to the cores, neither recycling nor re-sharpening was detected in the retouched flakes. Retouching was simple, and we rarely found scalar retouching, traditionally associated with bone retouchers. The same pattern has been observed at other sites such as Level J of Abric Romaní, where core reduction is maximised and retouching shows low-intensity use and reconfiguration (Vaquero et al., 2008). A recycling economy is also evident with some items that display a double patina, as well as a bone retoucher with dry fracture.

The presence of a deciduous tooth in Level N4 shows that the Neanderthal groups which inhabited the Prado Vargas cave spanned a range of ages including children and juveniles. This discovery is noteworthy because Neanderthal milk teeth have been analysed much less than permanent teeth. Furthermore, descriptions of lower dm1 are much less frequent than lower dm2 in the specialized literature. This lower dm1 will enhance our knowledge not only about this type of tooth but also about other Neanderthal deciduous teeth. This individual lower dm_1, with clear evidence of resorbed roots, was from a child who lost it *ante mortem* at the age of 9–10 years, and it was replaced by the first premolar (Schour and Massler, 19).

Morphologically, Prado Vargas 1360 is similar to dm1 specimens from Qesem Cave, Nadale 1, Sima de las Palomas, and Roc de Marsal in the presence of four cusps, an anterior fovea on the occlusal surface and a *tuberculum molare* (Arnold et al., 2016; Bayle et al., 2009; Hershkovitz et al., 2016; Trinkaus and Walker, 2017). These discrete traits have been identified in some Neanderthal lower dm1 (Bailey, 2002; Bailey and Hublin, 2006). However, without an EDJ analysis, the occlusal wear makes it difficult to confirm and compare other non-metric dental traits, such as the mid-trigonid crest between the protoconid and metaconid, or the existence of a posterior fovea. The linear dimensions of Prado Vargas 1360 confirm its taxonomical affinity with Neanderthals, as it matches the Neanderthal variation of the deciduous lower dm1. The crown area and the crown index of Prado Vargas also lie within the Neanderthal range of variation calculated in Table 7.

6. Conclusions

Prado Vargas cave preserves a detailed sedimentary sequence that enables the study of several Neanderthals occupation levels prior to the arrival of *Homo sapiens*. In this study we have presented the latest multi-disciplinary findings for Archaeological Level 4, contained in Unit PV4, which has been OSL and ^{14}C dated to MIS3, between 39.8-54.7 ka, indicating that it is an important assemblage for knowledge about the subsistence strategies and settlement patterns of late Neanderthal populations in the Iberian Peninsula. Prado Vargas is one of the essential sites for studying Neanderthal socio-economic and cultural dynamics prior to contact with *H. sapiens* and the interpretation of possible internal changes that may have contributed to their extinction. The Prado Vargas dm_1 specimen exhibits discrete anatomic traits and dimensions that fall within the existing variability range described for Neanderthals, and provide an important additional record of Neanderthal deciduous teeth for the Iberian Peninsula.

This cave site was visited recurrently by Neanderthal groups during the formation of Level 4, as well as during much earlier periods. Level 4 contains a succession of palimpsests of seasonal occupations, probably summer and autumn, when the cave floor was dry and was thus not waterlogged. The heavy anthropization of this level and the range of activities detected in it (butchering, woodwork, hide work and the presence of children), leads us to infer long-term occupations, probably complemented by other cave and outdoor sites. The recycling economy and the micro dimensions of the lithic assemblage can be interpreted as evidence of recurrent occupations, the cultural heritage of this regional group, or a combination of both factors.

Judging by the size of the cave, and bearing in mind its moisture levels, the site may have been inhabited by a small group during potentially recurrent seasonal occupations. The success of these occupations was dependent on knowledgeable exploitation of the natural environs around the site, where various activities were undertaken, both inside and outside the cave.

Our chronological, palaeoenvironmental and palaeoecological reconstructions reveal that the inhabitants of Prado Vargas were late Neanderthals who were adapted to the cold and may have already been living in small, separate groups with marked territories and cultural traditions. They lived at the site and in the surrounding area without contact with *H. sapiens*, and potentially survived some of the coldest stages of MIS 3 without completely abandoning this high elevation, inland region of the Cantabrian Ranges.

Author statement

Marta Navazo Ruiz: lithic technology. Marta Santamaría: lithic technology. Alfonso Benito-Calvo: geological setting and stratigraphy. Rodrigo Alonso-Alcalde: geological setting and stratigraphy. Pedro Alonso: zooarchaeology and bone retouchers. Héctor de la Fuente: zooarchaeology and taphonomy. Claudia Santamaría: traceology. Adrián Álvarez: microfaunal assamblage. Lee J. Arnold: OSL dating. Martina Demuro: OSL dating. Ma José Iriarte: pollen analysis. Marina Lozano: dental study. José Eugenio Ortiz: AAR dating. Trinidad Torres: AAR dating.

Declaration of competing interest

The authors declare that they have no known competing financial interests or personal relationships that could have appeared to influence the work reported in this paper.

Acknowledgements

Field work was supported by Consejería de Cultura y Turismo de la Junta de Castilla y León y Ayuntamiento Merindad de Sotoscueva. The C14 dating was funded by Fundación Palarq. The OSL dating research was funded by Australian Research Council (ARC) Discovery Early Career Researcher Award DE160100743 and ARC Future Fellowship project FT200100816 awarded to M. Demuro. Marta Santamaría is the beneficiary of a predoctoral grant from University of Burgos (UBU). Gala Gómez Merino did tasks of cleaning and conservation of the tooth. We are grateful to Fundación La Escuela (Cornejo), Asociación Naboki (Quisicedo), Casa del Parque del Monumento Natural de Ojo Guareña and Benigno Gómez Pereda.

Appendix A. Supplementary data

Supplementary data to this article can be found online at https://doi.org/10.1016/j.quascirev.2021.106795.

References

Alonso-García, P., Ruiz, M.N., Blasco, R., 2020. Use and selection of bone fragments in the north of the iberian Peninsula during the middle palaeolithic: bone retouchers from level 4 of Prado Vargas (Burgos, Spain). Archaeological and Anthropological Sciences 12 (9), 1–12. https://doi.org/10.1007/s12520-020-01097-z.

Altuna, J., 1971a. Los mamíferos del yacimiento prehistórico de Morín (Santander). J. González Echegaray, L.G. Freeman. In: Morín, Cueva (Ed.), Excavaciones 1966–68, Publicaciones del Patronato de Cuevas Prehistóricas de Santander 6, Santander, vol. 1971, pp. 367–398.

Altuna, J., 1971b. Los mamíferos del yacimientoprehistórico de Morín. In: González Echegaray, J., Freeman, L.G. (Eds.), Cueva Morín: Excavaciones, vols. 1966–1968. Patronato de las Cuevas Prehistóricas, Santander, pp. 367–398.

Altuna, J., 1973. Fauna de mamíferos de la Cueva de Morín. In: González Echegaray, J., Freeman, L.G. (Eds.), Cueva Morín: Excavaciones, vol. 1969. Patronato de las Cuevas Prehistóricas, Santander, pp. 281–290.

Altuna, J., 1980. Fauna de Axlor. Campaña de 1968, 69, 71 y 72. In: Barandiarán, J.M. (Ed.), Excavaciones en Axlor (Campaña de 1967-74). Obras completas, 17. Gran Enciclopedia Vasca.

Altuna, J., Mariezkurrena, K., 2000. Macromamíferos del yacimiento de Labeko Koba(Arrasate, País Vasco). In: Arrizabalaga, A., Altuna, J. (Eds.), Labeko Koba (PaísVasco). Hienas y humanos en los albores del Paleolítico Superior. Munibe(AntropologíaeArkeología), vol. 52, pp. 107–181.

Álvarez Lao, D.J., 2014. The Jou Puerta cave (Asturias, NW Spain): a MIS 3 large mammal assemblage with mixture of cold and temperate elements. Palaeogeography, Palaeoclimatology,. Palaeoecology 393, 1–1.

Andrews, P., Cook, J., 1990. Owls, Caves and Fossils: Predation, Preservation and Accumulation of Small Mammal Bones in Caves, with an Analysis of the Pleistocene Cave Faunas from Westbury-sub-Mendip. UK. University of Chicago Press, Somerset.

Andrews, P., Jalvo, Y.F., 1997. Surface modifications of the Sima de los Huesos fossil humans. J. Hum. Evol 33 (2–3), 191–217.

Arilla, M., Rosell, J., Blasco, R., Dominguez-Rodrigo, M., Pickering, T.R., 2014. The "bear" essentials: actualistic research on Ursus arctos arctos in the Spanish Pyrenees and its implications for paleontology and archaeology. PloS One 9 (7), e102457. https://doi.org/10.1371/journal.pone.0102457.

Arnaud, J., Benazzi, S., Romandini, M., Livraghi, A., Panetta, D., Salvadori, P.A., Peresani, M.A., 2016. Neanderthal deciduous human molar with incipient carious infection from the Middle Palaeolithic De Nadale cave, Italy. Am. J. Phys. Anthropol 162 (2), 370–376.

Arnold, L.J., Duval, M., Demuro, M., Spooner, N.A., Santonja, M., Pérez-González, A., 2016. OSL dating of individual quartz 'supergrains' from the Ancient Middle Palaeolithic site of Cuesta de la Bajada, Spain. Quat. Geochronol 36, 78–101. https://doi.org/10.1016/j.quageo.2016.07.003.

Arnold, L.J., Roberts, R.G., 2009. Stochastic modelling of multi-grain equivalent dose (De) distributions: implications for OSL dating of sediment mixtures. Quat. Geochronol 4 (3), 204–230. https://doi.org/10.1016/j.quageo.2008.12.001.

Arnold, L.J., Demuro, M., Ruiz, M.N., 2012. Empirical insights into multi-grain averaging effects from 'pseudo'single-grain OSL measurements. Radiat. Meas 47 (9), 652–658. https://doi.org/10.1016/j.radmeas.2012.02.005.

Arnold, L.J., Demuro, M., Navazo, M., Benito-Calvo, A., Pérez-González, A., 2013. OSL dating of the Middle Palaeolithic Hotel California site, Sierra de Atapuerca, north-central S pain. Boreas 42 (2), 285–305. https://doi.org/10.1111/j.1502-3885.2012.00262.x.

Arriaza, M.D.C., Huguet, R., Laplana, C., Pérez-González, A., Márquez, B., Arsuaga, J.L., Baquedano, E., 2017. Lagomorph predation represented in a middle Palaeolithic level of the Navalmaíllo Rock Shelter site (Pinilla del Valle, Spain), as inferred

via a new use of classical taphonomic criteria. Quat. Int 436, 294–306. https://doi.org/10.1016/j.quaint.2015.03.040.
Azorit, C., Analla, M., Carrasco, R., Calvo, J.A., Muñoz-Cobo, J., 2002. Teeth eruption pattern in red deer (Cervus elaphus hispanicus) in southern Spain. An. Biol 24, 2002.
Bailey, S.E., 2002. Neandertal Dental Morphology: Implications for Modern Human Origins. Doctoral dissertation. Arizona State University.
Bailey, S.E., Hublin, J.J., 2006. Dental remains from the grotte du Renne at arcy-sur-cure (Yonne). J. Hum. Evol 50 (5), 485–508. https://doi.org/10.1016/j.jhevol.2005.11.008.
Bargalló, A., Mosquera, M., Lorenzo, C., 2016. Identifying handedness at knapping; an analysis of the scatter pattern of lithic remains. Archaeol Anthropol Sci 10 (3), 587–598. https://doi.org/10.1007/s12520-016-0378-0.
Barone, R., 1976. Anatomie comparée des mammifères domestiques. Tome 1: ostéologie, 2ème éditi.
Bayle, P., Braga, J., Mazurier, A., Macchiarelli, R., 2009. Dental developmental pattern of the Neanderthal child from Roc de Marsal: a high-resolution 3D analysis. J. Hum. Evol 56 (1), 66–75. https://doi.org/10.1016/j.jhevol.2008.09.002.
Becerra-Valdivia, L., Leal-Cervantes, R., Wood, R., Higham, T., 2020. Challenges in sample processing within radiocarbon dating and their impact in 14C-dates-as-data studies. J. Archaeol. Sci 113, 105043. https://doi.org/10.1016/j.jas.2019.105043.
Bermúdez de Castro, J., Bromage, T.G., Jalvo, Y.F., 1988. Buccal striations on fossil human anterior teeth: evidence of handedness in the middle and early Upper Pleistocene. J. Hum. Evol 17 (4), 403–412. https://doi.org/10.1016/0047-2484(88)90029-2.
Binford, L.R., 1981. Bones: Ancient Men and Modern Myths. Academic Press, New York, p. 320.
Bird, M.I., Ayliffe, L.K., Fifield, L.K., Turney, C.S., Cresswell, R.G., Barrows, T.T., David, B., 1999. Radiocarbon dating of "old" charcoal using a wet oxidation, stepped- combustion procedure. Radiocarbon 41 (2), 127–140. https://doi.org/10.1017/S0033822200019482.
Bird, M.I., Levchenko, V., Ascough, P.L., Meredith, W., Wurster, C.M., Williams, A., Apperley, D.C., 2014. The efficiency of charcoal decontamination for radiocarbon dating by three pre-treatments–ABOX, ABA and hypy. Quat. Geochronol 22, 25–32. https://doi.org/10.1016/j.quageo.2014.02.003.
Blumenschine, R.J., 1995. Percussion marks, tooth marks, and experimental determinations of the timing of hominid and carnivore access to long bones at FLK Zinjanthropus, Olduvai Gorge, Tanzania. J. Hum. Evol 29 (1), 21–51. https://doi.org/10.1006/jhev.1995.1046.
Bourguignon, L., Faivre, J.P., Turq, A., 2004. Ramification des chaînes opératoires: une spécificité du Moustérien. Paléo 16, 37–48.
Bowler, J.M., Johnston, H., Olley, J.M., Prescott, J.R., Roberts, R.G., Shawcross, W., Spooner, N.A., 2003. New ages for human occupation and climatic change at Lake Mungo, Australia. Nature 421 (6925), 837–840. https://doi.org/10.1038/nature01383.
Brain, C.K., 1969. The contribution of Namib Desert Hottentots to an understanding of australopithecine bone accumulations. Scientific Papers of the Namib Desert Research Station 1969 (39), 13–22.
Brain, C.K., 1981. The Hunters or the Hunted?: an Introduction to African Cave Taphonomy. University of Chicago Press.
Brock, F., Higham, T.F.G., 2009. AMS radiocarbon dating of Paleolithic-aged charcoal from Europe and the Mediterranean Rim using ABOx-SC. Radiocarbon 51 (2), 839–846. https://doi.org/10.1017/S0033822200056149.
Bromage, T.G., 1984. Interpretation of scanning electron microscopic images of abraded forming bone surfaces. Am. J. Phys. Anthropol 64 (2), 161–178. https://doi.org/10.1002/ajpa.1330640210.
Brooks, A.S., Hare, P.E., Kokis, J.E., Durana, K., 1991. A burning question: differences in laboratory induced and natural diagenesis in ostrich eggshell proteins. Annual Report of the Geophysical Laboratory, Carnegie Institution of Washington 176–179.
Bunn, H.T., 1983. Comparative analysis of modern bone assemblages from a San hunter- gatherer camp in the Kalahari Desert, Botsuwana, and from a spotted hyena den near Nairobi, Kenya. Animal and Archaeology, 1. Hunters and Their Prey. BAR Int. Ser 163, 141–148.
Bunn, H.T., 1986. Patterns of skeletal representation and hominid subsistence activities at Olduvai Gorge, Tanzania, and Koobi Fora, Kenya. J. Hum. Evol 15 (8), 673–690. https://doi.org/10.1016/S0047-2484(86)80004-5.
Burjachs, F., López-Sáez, J.A., Iriarte, M.J., 2003. Metodología arqueopalinológica. La recogida de muestras en arqueobotànica: objetivos y propuestas metodológicas 11–18.
Carbonell, E., Guilbaud, M., Mora, R., 1983. Utilización de la lógica analítica para el estudio de tecno-complejos a cantos tallados. Cahier Noir 1, 1–64.
Carbonell, E., Rodríguez, X.P., Sala, R., Vaquero, M., 1992. New elements of the logical analytic system first." international meeting on technical systems to configure lithic objects of scarce elaboration. Cahier Noir 6, 3–61.
Carlsen, O., 1987. Dental Morphology. Copenhagen: Munksgaard Ed, p. 194.
Carmignani, L., Moncel, M.H., Fernandes, P., Wilson, L., 2017. Technological variability during the early middle palaeolithic in western Europe. Reduction systems and predetermined products at the Bau de l'Aubesier and Payre (South-East France). PloS one 12 (6). https://doi.org/10.1371/journal.pone.0178550 e0178550.
Carrión, E., Baena, J., Conde, C., Cuartero, F., y Roca, M., 2008. Variabilidad tecnológica en el musteriense de Cantabria. Treballs d'Arqueolgia 14, 279–318.
Carrión, J.S., Fernández, S., Jiménez-Arenas, J.M., Munuera, M., Ochando, J., Amorós, G., Hajdas, I., 2019. The sequence at Carihuela Cave and its potential for research into Neanderthal ecology and the Mousterian in southern Spain. Quat. Sci. Rev 217, 194–216. https://doi.org/10.1016/j.quascirev.2019.04.012.
Castaños, P., 1996. Hallazgos de rinoceronte lanudo en Legintxiki (Etxauri, Navarra).Principe de Viana. Suplemento de Ciencias 14/15 77–80.
Castaños, P., 2005. Revisión actualizada de las faunas de macromamíferos del Würmantiguo en la Región Cantábrica. Museo de Altamira. Monografías 20, 201–207.
Chaline, J., 1972. Les rongeurs du Pléistocène moyen et supérieur de France: (systématique, biostratigraphie, paléoclimatologie).
Chaline, J., 1974. Les proies des rapaces (petits Mammifères et leur environnement). Doin éditions, Paris.
Costamagno, S., Bourguignon, L., Soulier, M., Meignen, L., Beauval, C., Rendu, W., Maureille, B., 2018. Bone retouchers and site function in the Quina mousterian: the case of les Pradelles (Marillac-le-Franc, France). In: Hutson, J.M., García-Moreno, A., Noack, E.S., Turnet, E., Villaluenga, A., Gaudzinski-Windheuser, S. (Eds.), The Origin of Bone Tool Technologies. "Retouching the Palaeolithic: Becoming Human and the Origins of Bone Tool Technology", Conference at Schloss Herrenhausen in Hannover, Germany, 21-23 October 2015. RGZM-TAGUNGEN, Hannover, Germany, pp. 165–196. https://doi.org/10.11588/propylaeum.408.
Couto, M.A., Sánchez, G., Tavares, C.D., Barceló, A.M., Nunes, L.F., Herráez, C.F., Pires, V., Marques, J., Mendes, L., Chazarra, A., Cunha, S., Mendes, M., Neto, J., Silva, A., 2011. Atlas climático ibérico. Instituto de Meteorologia de Portugal and Agencia Estatal de Meteorología, Ministerio de Medio Ambiente y Medio Rural y Marino: Madrid, Spain, vol. 2011, p. 80.
Crisp, M.K., 2013. Amino Acid Racemization Dating: Method Development Using African Ostrich (Struthio camelus) Eggshell (Doctoral dissertation. University of York.
Cuartero, F., 2007. Tecnología lítica en Cova Bolomor IV: ¿una economía de reciclado? Saguntum 39, 27–44.
Cuenca-Bescós, G., Straus, L.G., Morales, M.R.G., Pimienta, J.C.G., 2009. The reconstruction of past environments through small mammals: from the mousterian to the bronze age in el mirón cave (Cantabria, Spain). J. Archaeol. Sci 36 (4), 947–955. https://doi.org/10.1016/j.jas.2008.09.025.
Cuenca-Bescós, G., Straus, L.G., García-Pimienta, J.C., Morales, M.G., López-García, J., M, 2010. Late quaternary small mammal turnover in the cantabrian region: the extinction of pliomys lenki (rodentia, mammalia). Quat. Int 212 (2). https://doi.org/10.1016/j.quaint.2009.06.006, 129–13.
del Olmo Zamora, P., Ramírez del Pozo, J., Aguilar Tomás, M.J., Portero García, J.M., y Olive Davó, A., 1918. Mapa Geológico de España e. 1:50.000. Hoja 84 (19-06), Espinosa de los Monteros». 1:50.000. Serie Magna. Madrid: IGME.
Delagnes, A., Rendu, W., 2011. Shifts in Neanderthal mobility, technology and subsistence strategies in western France. J. Archaeol. Sci 38 (8), 1771–1783.
Delaney-Rivera, C., Plummer, T.W., Hodgson, J.A., Forrest, F., Hertel, F., Oliver, J.S., 2009. Pits and pitfalls: taxonomic variability and patterning in tooth mark dimensions. J. Archaeol. Sci 36 (11), 2597–2608. https://doi.org/10.1016/j.jas.2009.08.001.
Delpiano, D., Heasly, K., Peresani, M., 2018. Assessing Neanderthal land use and lithic raw material management in Discoid technology. JASs Reports. Journal of Anthropological Sciences 96, 1–22.
Demuro, M., Arnold, L.J., Froese, D.G., Roberts, R.G., 2013. OSL dating of loess bracketing Sheep Creek tephra beds, northwest Canada: dim and problematic single-grain OSL characteristics and their effect on multi-grain age estimates. Quat. Geochronol 15, 67–87. https://doi.org/10.1016/j.yqres.2011.11.009.
Demuro, M., Arnold, L.J., Parés, J.M., Sala, R., 2015. Extended-range luminescence chronologies suggest potentially complex bone accumulation histories at the Early-to-Middle Pleistocene palaeontological site of Huéscar-1 (Guadix-Baza basin, Spain). Quat. Int 389, 191–212. https://doi.org/10.1016/j.quaint.2014.08.035.
Demuro, M., Arnold, L.J., Aranburu, A., Sala, N., Arsuaga, J.L., 2019. New bracketing luminescence ages constrain the Sima de los Huesos hominin fossils (Atapuerca, Spain) to MIS 12. J. Hum. Evol 131, 76–95. https://doi.org/10.1016/j.jhevol.2018.12.003.
Devièse, T., Karavanić, I., Comeskey, D., Kubiak, C., Korlević, P., Hajdinjak, M., Higham, T., 2017. Direct dating of neanderthal remains from the site of Vindija cave and implications for the middle to upper paleolithic transition. Proc. Natl. Acad. Sci. Unit. States Am 114 (40), 10606–10611. https://doi.org/10.1073/pnas.1709235114.
Dominguez-Ballesteros, Arrizabalaga, 2014. Laterality in the first neolithic and chalcolithic farming communities in northern Iberia, laterality: asymmetries of body, brain and cognition. https://doi.org/10.1080/1357650X.2014.982130.
Dominguez-Ballesteros, E., Arrizabalaga, A., 2015a. Flint knapping and determination of human handedness. Methodological proposal with quantifiable results. Journal of Archaeological Science: Report 3, 313–320. https://doi.org/10.1080/1357650X.2014.982130.
Dominguez-Ballesteros, E., Arrizabalaga, A., 2015b. Laterality in the first Neolithic and Chalcolithic farming communities in northern Iberia. Laterality 20(3) 371387. https://doi.org/10.1016/j.jasrep.2015.06.026.
Domínguez-Rodrigo, M., 1997. Meat-eating by early hominids at the FLK 22Zinjanthropussite, Olduvai Gorge (Tanzania): an experimental approach using cut-mark data. J. Hum. Evol 33 (6), 669–690. https://doi.org/10.1016/j.quascirev.2019.106008.
Domínguez-Rodrigo, M., 2002. Hunting and scavenging by early humans: the state of the debate. J. World PreHistory 16 (1), 1–54. https://doi.org/10.1023/A:

1014507129795.
Domınguez-Rodrigo, M., Piqueras, A., 2003. The use of tooth pits to identify carnivore taxa in tooth-marked archaeofaunas and their relevance to reconstruct hominid carcass processing behaviours. J. Archaeol. Sci 30 (11), 1385–1391. https://doi.org/10.1016/S0305-4403(03)00027-X.
Douka, K., Higham, T., Sinitsyn, A., 2010. The influence of pretreatment chemistry on the radiocarbon dating of Campanian Ignimbrite-aged charcoal from Kostenki 14 (Russia). Quat. Res 73 (3), 583–587. https://doi.org/10.1016/j.yqres.2010.01.002.
d'Errico, F., Sánchez Goñi, M.F., 2003. Neandertal extinction and the millennial scale climatic variability of OIS 3. Quat. Sci. Rev 22, 769–788.
Faerman, M., Zilberman, U., Smith, P., Kharitonov, V., Batsevitz, V., 1994. A neanderthal infant from the barakai cave, western Caucasus. J. Hum. Evol 27 (5), 405–415. https://doi.org/10.1006/jhev.1994.1056.
Faivre, J.-P., Discamps, E., Gravina, B., Turq, A., Guadelli, J.-L., Lenoir, M., 2014. The Contribution of Lithic Production Systems to the Interpretation of Mousterian Industrial Variability in South-Western France: the Example of Combe-Grenal (Dordogne, France). Quaternary International.
Fernández, M.H., 2001. Bioclimatic discriminant capacity of terrestrial mammal faunas. Global Ecol. Biogeogr 10 (2), 189–204. https://doi.org/10.1046/j.1466-822x.2001.00218.x.
Fernández, M.H., Peláez-Campomanes, P., 2005. Quantitative palaeoclimatic inference based on terrestrial mammal faunas. Global Ecol. Biogeogr 14 (1), 39–56. https://doi.org/10.1111/j.1466-822X.2004.00125.x.
Fernández, M.H., Sierra, M.Á.Á., Peláez-Campomanes, P., 2007. Bioclimatic analysis of rodent palaeofaunas reveals severe climatic changes in Southwestern Europe during the Plio- Pleistocene. Palaeogeography, Palaeoclimatology. Palaeoecology 251 (3–4), 500–526. https://doi.org/10.1016/j.palaeo.2007.04.015.
Fernandez-Jalvo, Y., Andrews, P., 2016. Atlas of Taphonomic Identifications: 1001+ Images of Fossil and Recent Mammal Bone Modification. Springer.
Fernández-Jalvo, Y., Andrews, P., Denys, C., Sesé, C., Stoetzel, E., Marin-Monfort, D., Pesquero, D., 2016. Taphonomy for taxonomists: implications of predation in small mammal studies. Quat. Sci. Rev 139, 138–157. https://doi.org/10.1016/j.quascirev.2016.03.016.
Fisher, J.W., 1995. Bone surface modifications in zooarchaeology. J. Archaeol. Method Theor 2 (1), 7–68.
Frayer, D.W., Clarke, R.J., Fiore, I., Blumenschine, R.J., Perez-Perez, A., Martinez, L.M., Bondioli, L., 2016. OH-65: the earliest evidence for right-handedness in the fossil record. J. Hum. Evol 100, 65–72. https://doi.org/10.1080/1357650X.2010.529451.
Fuentes Vidarte, C., 1980. Estudio de la fauna de "El Pendo". In: González Echegaray, En J. (Ed.), El Yacimiento de la Cueva de "El Pendo".Madrid: Bibliotheca Praehistorica Hispana, vol. 17, pp. 215–237.
Galbraith, R.F., Roberts, R.G., Laslett, G.M., Yoshida, H., Olley, J.M., 1999. Optical dating of single and multiple grains of quartz from Jinmium rock shelter, northern Australia: Part I, experimental design and statistical models. Archaeometry 41 (2), 339–364. https://doi.org/10.1111/j.1475-4754.1999.tb00987.x.
Harvati-Papatheodorou, K., 2013. Neanderthals. A companion to paleoanthropology. In: Begun, D. (Ed.), Wiley Blackwell, pp. 538–556.
Haynes, G., 1980. Evidence of carnivore gnawing on Pleistocene and Recent mammalian bones. Paleobiology 341–351. https://doi.org/10.2307/2400350.
Haynes, G., 1983. Frequencies of spiral and green-bone fractures on ungulate limb bones in modern surface assemblages. Am. Antiq 102–114. https://doi.org/10.2307/279822.
Hershkovitz, I., Weber, G.W., Fornai, C., Gopher, A., Barkai, R., Slon, V., Sarig, R., 2016. New middle Pleistocene dental remains from Qesem cave (Israel). Quat. Int 398, 148–158. https://doi.org/10.1016/j.quaint.2015.08.059.
Higham, T., 2011. European Middle and Upper Palaeolithic radiocarbon dates are often older than they look: problems with previous dates and some remedies. Antiquity 85 (327), 235–249. https://doi.org/10.1017/S0003598X00067570.
Higham, T., Brock, F., Peresani, M., Broglio, A., Wood, R., Douka, K., 2009. Problems with radiocarbon dating the middle to upper palaeolithic transition in Italy. Quat. Sci. Rev 28 (13–14), 1257–1267. https://doi.org/10.1016/j.quascirev.2008.12.018.
Higham, H., Douka, K., Wood, R., Bronk, C., Brock, F., Basell, F., Camps, M., Arrizabalaga, A., Baena, J., Barroso, C., Bergman, C., Boitard, C., Boscato, P., Caparrós, M., Conard, N.J., Draily, C., Froment, A., Galván, B., Gambassini, P., Garcia-M, A., Grimaldi, S., Haesaerts, P., Holt, B., Iriarte, Ma J., Jelinek, A., Jorda, J.F., Maillo, J.M., Marom, A., Maroto, J., Menéndez, M., Metz, L., Morin, M., Moroni, A., Negrino, F., Panagopoulou, E., Peresani, M., Pirson, S., e la Rasilla, M., Riel-Salvatore, J., Ronchitelli, A., Santamaria, D., Semal, P., Slimak, L., Soler, J., Soler, N., Villaluenga, A., Pinhasi, R., Jacobi, R., 2014. The timing and spatiotemporal patterning of Neanderthal disappearance 512 (7514), 306–309. https://doi.org/10.1038/nature13621.
Hublin, J.J., 2013. Free digital scans of human fossils. Nature 497 (7448). https://doi.org/10.1038/497183a, 183–183.
Hublin, J.J., Sirakov, N., Aldeias, V., Bailey, S., Bard, E., Delvigne, V., Endarova, E., Fagault, Y., Fewlass, H., Hajdinjak, M., Kromer, B., Krumov, I., Marreiros, J., Martisius, N.L., Paskulin, L., Sinet-Mathiot, V., Meyer, M., Pääbo, S., Popov, Z., Rezek, V., Sirakova, S., Skinner, M., Smith, G.M., Spasov, R., Talamo, S., Tuna, T., Wacker, L., Welker, F., Wilcke, A., Zahariev, N., McPherron, S.P., Tsanova, T., 2020. Initial upper palaeolithic Homo sapiens from Bacho Kiro cave, Bulgaria. Nature 1–4. https://doi.org/10.1038/s41586-020-2259-z.
Iriarte-Chiapusso, M.J., Wood, R., Sáenz de Buruaga, A., 2019. Arrillor cave (Basque Country, northern Iberian Penisula). Chronological, palaeo-environmental and cultural notes on a long Mousterian sequence. Quat. Int 508, 107–115.
Jiménez-Espejo, F.J., Martínez-Ruiz, F., Finlayson, C., Paytan, A., Sakamoto, T., OrtegaHuertas, M., Finlayson, G., Iijima, K., Gallego-Torres, D., Fa, D., 2007. Climate forcing and Neanderthal extinction in Southern Iberia: insights from a multiproxy marine record. Quat. Sci. Rev 26, 836–852.
Jiménez-Sánchez, M., Rodríguez-Rodríguez, L., García-Ruiz, J.M., Domínguez-Cuesta, M.J., Farias, P., Valero-Garcés, B., Valcárcel, M., 2013. A review of glacial geomorphology and chronology in northern Spain: timing and regional variability during the last glacial cycle. Geomorphology 196, 50–64. https://doi.org/10.1016/j.geomorph.2012.06.009.
Jones, J.R., Richards, M.P., Straus, L.G., Reade, H., Altuna, J., Mariezkurrena, K., MarínArroyo, A.B., 2018. Changing environments during the Middle-Upper Palaeolithic transition in the eastern Cantabrian Region (Spain): direct evidence from stable isotope studies on ungulate bones. Sci. Rep 8. https://doi.org/10.1038/s41598018-32493-0, 14842.
Kaufman, D.S., Manley, W.F., 1998. A new procedure for determining DL amino acid ratios in fossils using reverse phase liquid chromatography. Quat. Sci. Rev 17 (11), 987–1000. https://doi.org/10.1016/S0277-3791(97)00086-3.
Krause, J., Orlando, L., Serre, D., Viola, B., Prüfer, K., Richards, M.P., Hublin, J.-J., Hänni, C., Derevianko, P., Pääbo, S., 2007. Neanderthals in central Asia and Siberia. Nature 449 (7164), 902–904. https://doi.org/10.1038/nature06193.
Lafont, R., Périnet, G., Bazile, F., Icole, M., 1984. Racémisation d'acides aminés d'ossements fossiles du Paléolithique supérieur languedocien. Comptes-rendus des séances de l'Académie des sciences. Série 2, Mécanique-physique. chimie, sciences de l'univers, sciences de la terre 299 (8), 447–450.
Lalueza, C., 2020. Grabado en los genes. Muy interesante 19–25.
Luret, M., Burke, A., Bernaldo de Quiros, F., Besse, M., 2020. El Castillo cave (Cantabria, Spain): archeozoological comparison between the Mousterian occupation level (unit 20) and the "Aurignacien de transition de type El Castillo" (unit 18). Journal of Archaeological Science. Report 31, 102339.
Lyman, R.L., 2008. Quantitative Paleozoology. Cambridge University Press, p. 348.
Lyman, R.L., Lyman, C., 1994. Vertebrate Taphonomy. Cambridge University Press, p. 552.
Machado, J., Hernández, C.M., Mallol, C., Galván, B., 2013. Lithic production, site formation and Middle Palaeolithic palimpsest analysis: in search of human occupation episodes at Abric del Pastor stratigraphic unit iv (Alicante, Spain). J. Archaeol. Sci 40 (5), 2254–2273.
Madrid Sepulchre, P., Ramstein, G., Kageyama, M., Vanhaeren, M., Krinner, G., Sanchez-Goni, M.-F., dErrico, F., 2007. H4 abrupt event and late Neanderthal presence in Iberia. Earth Planet Sci. Lett 258, 283–292.
Maillo, J.M., 2007. Aproximación tecnológica del final del Musteriense de Cueva Morín (Villanueva de Villaescusa, Cantabria, España). Munibe 58, 1342.
Mallye, J.B., Thiébaut, C., Mourre, V., Costamagno, S., Claud, É., Weisbecker, P., 2012. The Mousterian bone retouchers of Noisetier Cave: experimentation and identification of marks. J. Archaeol. Sci 39 (4), 1131–1142. https://doi.org/10.1016/j.jas.2011.12.018.
Martellotta, E.F., Delpiano, D., Govoni, M., Nannini, N., Duches, R., Peresani, M., 2020. The use of bone retouchers in a Mousterian context of Discoid lithic technology. Archaeological and Anthropological Sciences 12 (9). https://doi.org/10.1007/s12520-020-01155-6.
Marzin, E., 1990. Essai de normalisation du protocole d'analyse des taux de racemisation des acides amines: applications a la datation d'ossements fossiles. Travaux du LAPMO 8, 167–178.
Menéndez, M., Álvarez-Alonso, D., Andrés-Herrero, M., de Carral, P., García, Sánchez, E., Jordá-Pardo, J.F., Quesada, J.M., Rojo, J., 2018. The middle to upper paleolithic transition in La Güelga cave (Asturias,NorthernSpain). Quat. Int 474, 71–84.
Mizoguchi, Y, 2002. Dental remains excavated at the Dederiyeh Cave during the 1989-1994 seasons. In: Akazara, T., Muhesen, S. (Eds.), Neanderthal Burials. Excavations of the Dederiyeh Cave, Afrin, Syria. Pp.221-262. Japan. University of Tokio.
Molnar, S., 1971. Human tooth wear, tooth function and cultural variability. Am. J. Phys. Anthropol 34 (2), 175–189. https://doi.org/10.1002/ajpa.1330340204.
Moncel, M.-H. e. a, 1998. Halte de chasse au chamois au Paléolithique moyen: la couche 5 de Capitulo X: bibliografía 555 la grotte Sclandina (Sclayn, Namur, Belgique). En: Économie préhistorique: les comportements de subsistance au Paléolithique. XVIII Rencontres Internationales d'Archeologie et d'Histoire d'Antibes 291–308.
Moncel, M.-H., Fernandes, P., Willmes, M., James, H., Grün, R., 2019. Rocks, teeth, and tools: new insights into early Neanderthal mobility strategies in South-Eastern France from lithic reconstructions and strontium isotope analysis. PloS One 14 (4). https://doi.org/10.1371/journal.pone.0214925 e0214925.
Mourre, V., Thiébaut, C., 2008. L'industrie lithique du moustérien final de la Grotte du Noisetier (Fréchet- Aure, Hautes-Pyrénées) dans le contexte des Pyrénées centrales française. In: Mora Torcal, R., Martinez Moreno, J., De la Torre Sainz, I., Casanova Marti, J. (Eds.), Treballs d'Arqueologia, Universitat Autonoma de Barcelona, Cente d'Estudis del Patrimoni Arqueologico de la Préhistoria, 14, Variabilidad técnica del Paleolitico Médio en el sudoeste de l'Europa, pp. 87–104.
Mozota Holgueras, M., 2012. El hueso como materia prima: El utillaje óseo del final del Musteriense en el sector central del norte de la Península Ibérica. Doctoral dissertation. Universidad de Cantabria.
Murray, A.S., Wintle, A.G., 2000. Luminescence dating of quartz using an improved single-aliquot regenerative-dose protocol. Radiat. Meas 32 (1), 57–73. https://

doi.org/10.1016/S1350-4487(99)00253-X.
Navazo, M., Carbonell, E., 2014. Neanderthal settlement patterns during MIS 4–3 in Sierra de Atapuerca (Burgos, Spain).Quaternary International, vol. 331, pp. 267–277. https://doi.org/10.1016/j.quaint.2014.03.032.
Navazo, M., Díez, J.C., 2008. Prado Vargas y la variabilidad tecnológica a finales del Paleolítico Medio en la meseta norte. Treballs arqueol 14, 121–139.
Navazo, M., Fernández-Lomana, J.C.D., de Torres Pérez-Hidalgo, T., Colina, Á., Menéndez, J.E.O., 2005. La Cueva del Prado Vargas: un yacimiento del Paleolítico Medio en el Sur de la Cordillera Cantábrica. In Neandertales cantábricos, estado de la cuestión: actas de la reunión científica: celebrada en el Museo de Altamira los días 20-22 de octubre de 2004, 151–166. Subdirección General de Publicaciones, Información y Documentación.
Navazo Ruiz, M., Jordá Pardo, J.F., Burow, C., Kehl, M., Pastoors, A., Weniger, G.C., Wood, R., 2020. Last Neanderthal Occupations at Central Iberia: the Lithic Industry of Jarama VI Rock Shelter (Valdesotos, Guadalajara, Spain). https://doi.org/10.1007/s12520-019-00974-6.
Nilssen, P.J., 2000. An Actualistic Butchery Study in South Africa and its Implications for Reconstructing Hominid Strategies of Carcass Acquisition and Butchery in the Upper Pleistocene and Plio-Pleistocene. Ph.D. Dissertation. University of Cape Town.
Olsen, S.L., Shipman, P., 1988. Surface modification on bone: trampling versus butchery. J. Archaeol. Sci 15 (5), 535–553. https://doi.org/10.1016/0305-4403(88)90081-7.
Ortega, A.I., Martin, M.A., Edelweiss, G., 2013. Cuevas de Ojo Guareña. Una visión de la mano del Grupo Espeleológico Edelweiss.
Ortiz, J.E., Sánchez-Palencia, Y., Gutiérrez-Zugasti, I., Torres, T., González-Morales, M., 2020. Mimicking the effects of anthropogenic heating on amino acid racemisation dating of gastropod shells. Quat. Geochronol 101084. https://doi.org/10.1016/j.quageo.2020.101084.
Otte, M., 1998. “Industrie Lithique de la Couche 5”. En VV.AA.: Recherches aux Grottes de Sclayn, vol. 2. L'Archeologie. ERAUL, pp. 277–278, 79. Lieja.
Pike-Tay, A., Cabrera Valdés, V., Bernaldo de Quirós, F., 1999. Seasonal variations of the middle-upper paleolithic transition at El castillo, Cueva Morín and El pendo (Cantabria, Spain). J. Hum. Evol 36 (3), 283–317.
Pinhasi, R., Higham, T.F., Golovanova, L.V., Doronichev, V.B., 2011. Revised age of late Neanderthal occupation and the end of the Middle Paleolithic in the northern Caucasus. In: Proceedings of the National Academy of Sciences of the United States of America, vol. 108, pp. 8611–8616. https://doi.org/10.1073/pnas.1018938108, 21.
Prescott, J.R., Hutton, J.T., 1994. Cosmic ray contributions to dose rates for luminescence and ESR dating: large depths and long-term time variations. Radiat. Meas 23 (2–3), 497–500. https://doi.org/10.1016/1350-4487(94)90086-8.
Ramsey, C.B., 2009. Bayesian analysis of radiocarbon dates. Radiocarbon 51 (1), 337–360. https://doi.org/10.1017/S0033822200033865.
Reimer, P.J., Bard, E., Bayliss, A., Beck, J.W., Blackwell, P.G., Bronk Ramsey, C., Buck, C.E., Cheng, H., Edwards, R.L., Friedrich, M., Grootes, P.M., Guilderson, T.P., Haflidason, H., Hajdas, I., Hatté, C., Heaton, T.J., Hoffmann, D.L., Hogg, A.G., Hughen, K.A., Kaiser, K.F., Kromer, B., Manning, S.W., Niu, M., Reimer, R.W., Richards, D.A., Scott, E.M., Southon, J.R., Staff, R.A., Turney, C.S.M., van der Plicht, J., 2013. IntCal13 and Marine13 radiocarbon age calibration curves 0–50.000 years cal BP. Radiocarbon 55 (4), 1869–1887. https://doi.org/10.2458/azu_js_rc.55.16947.
Reitz, E.J., Reitz, E., Wing, E.S., 1999. Zooarchaeology. Cambridge University Press.
Rigaud, A., 1977. Analyse typologique et technologique des grattoirs magdaléniens de La Garenne à Saint-Marcel (Indre), Gallia préhistoire. t.20 f.1 1–43. https://doi.org/10.3406/galip.1977.
Ríos, J., 2005. Características de la producción lítica al final del Paleolítico Medio en el País Vasco: el caso del nivel B de Axlor (Dima, Bizkaia). In Neandertales cantábricos, estado de la cuestión: actas de la reunión científica: celebrada en el Museo de Altamira los días 20-22 de octubre de 2004, 333–348 (Subdirección General de Publicaciones, Información y Documentación).
Ríos, J., Eixea, A., Villaverde, V., 2015. Ramification of lithic production and the search of small tools in Iberian Peninsula Middle Paleolithic. Quat. Int 361, 188–199.
Rodríguez, X.P., Hedges, J.W., 2004. Technical systems of lithic production in the Lower and Middle Pleistocene of the Iberian Peninsula: technological variability between northeastern sites and Sierra de Atapuerca sites, vol. 1323. British Archaeological Reports.
Román, J., 2019. Manual para la identificación de los cráneos de los roedores de la península ibérica, islas baleares y canarias. Manuales de Mastozoología de la SECEM.
Sánchez-Fernández, G., y Bernaldo de Quirós, F., 2008. El final del Musteriense cantábrico: el nivel 20e de la cueva de El Castillo (Cantabria). Férvedes 5, 117–126.
Sánchez-Hernández, C., Rivals, F., Blasco, R., Rosell, J., 2014. Short, but repeated Neanderthal visits to Teixoneres Cave (MIS 3, Barcelona, Spain): a combined analysis of tooth microwear patterns and seasonality. J. Archaeol. Sci 49, 317–325.
Santamaría, C., Luengo, S.M., Navazo, M., Benito-Calvo, A., Martín, I., 2016. Aproximación metodológica y primeros resultados sobre huellas de uso en herramientas de sílex del yacimiento musteriense de Prado Vargas (Cornejo, Burgos, España), a través de microscopio confocal. Digit 3, 15–22. https://doi.org/10.14195/2182-844X_3.
Santamaría, M., Navazo, M., Benito-Calvo, A., Alonso, R., López, G., Carbonell, E., 2020. Atapuerca neanderthal landscape at fuente mudarra site in Burgos, Spain, during marine isotope stages 5 – 3. Quat. Res. https://doi.org/10.1017/qua.2020.65. In press.
Schour, I., Massler, M., 1944. Development of the human dentition, distributed by the American dental association.
Scott, G.R., Turner, I.I.C.G., 1997. The Anthropology of Modern Human Teeth. Dental Morphology and its Variation in Recent Human Populations. Cambridge University Press, p. 382.
Selvaggio, M.M., Wilder, J., 2001. Identifying the involvement of multiple carnivore taxa with archaeological bone assemblages. J. Archaeol. Sci 28 (5), 465–470. https://doi.org/10.1006/jasc.2000.0557.
Semenov, S.A., 1981. Prehistorictechnolog Y. Akal Universitaria.
Shipman, P., 1981. Life History of a Fossil: an Introduction to Taphonomy and Paleoecology, 56.012 SHI.
Shipman, P., Rose, J., 1983. Early hominid hunting, butchering, and carcass-processing behaviors: approaches to the fossil record. J. Anthropol. Archaeol 2 (1), 57–98. https://doi.org/10.1016/0278-4165(83)90008-9.
Shipman, P., Foster, G., Schoeninger, M., 1984. Burnt bones and teeth: an experimental study of color, morphology, crystal structure and shrinkage. J. Archaeol. Sci 11 (4), 307–325.
Slimak, L., 1999. Pour une individualisation des Moustériens de type Quina dans le quart sudest de la France? La Baume Néron (Soyons, Ardèche) et le Champ Grand (Saint-Maurice-surLoir, Loire), premières données. Bull. Soc. Prehist. Fr 96 (2), 133144.
Slon, V., Mafessoni, F., Vernot, B., de Filippo, C., Grote, S., Viola, B., Hajdinjak, M., Peyrégne, S., Nage, S., Brown, S., Douka, K., Higham, T., Kozlikin, M.B., Shunkov, M.V., Derevianko, A.P., Kelso, J., Meyer, M., Prüfer, K., Pääbo, S., 2018. The genome of the offspring of a Neanderthal mother and a Denisovan father. Nature 561 (7721), 113–116. https://doi.org/10.1038/s41586-018-0455-x.
Stiner, M.C., Kuhn, S.L., Weiner, S., Bar-Yosef, O., 1995. Differential burning, recrystallization, and fragmentation of archaeological bone. J. Archaeol. Sci 22 (2), 223–237.
Torres, T., Ortiz, J.E., Fernández, E., Arroyo-Pardo, E., Grün, R., Pérez-González, A., 2014. Aspartic acid racemization as a dating tool for dentine: a reality. Quat. Geochronol 22, 43–56. https://doi.org/10.1016/j.quageo.2014.02.004.
Trinkaus, E., Walker, M.J. (Eds.), 2017. The people of Palomas. Neandertals from the Sima de las Palomas del Cabezo Gordo, Southeastern Spain. Texas. Texas A&M University Press, p. 278.
Trinkaus, E., Moldovan, O., Milota, S., Bîlgăr, A., Sarcina, L., Athreya, S., Bailey, S.E., Rodrigo, R., Mircea, G., Higham, T., Ramsey, C.B., van der Plicht, J., 2003. An early modern human from the Peştera cu Oase, Romania. Proc. Natl. Acad. Sci. U. S. A 100 (20), 11231–11236. https://doi.org/10.1016/j.jhevol.2003.08.003.
Turq, A., Faivre, J.P., Gravina, B., Bourguignon, L., 2017. Building models of Neanderthal territories from raw material transports in the Aquitaine Basin (southwestern France). Quat. Int 433, 88–101.
Uomini, N.T., 2011. Handedness in Neanderthals. In: Conard, N.J., Richter, J. (Eds.), Neanderthal Lifeways, Subsistence and Technology. Springer, Netherlands, Dordrecht, pp. 139–154. https://doi.org/10.1007/978-94-007-0415-2_14.
Vallejo, S., Urtiaga, K., Navazo, M., 2017. Characterization and supply of raw materials in the Neanderthal groups of Prado Vargas Cave (Cornejo, Burgos, Spain). Q. Int 435, 35–48. https://doi.org/10.1016/j.quaint.2015.09.054.
Verna, C., d'Errico, F., 2011. The earliest evidence for the use of human bone as a tool. J. Hum. Evol 60 (2), 145–157. https://doi.org/10.1016/j.jhevol.2010.07.027.
Villa, P., Mahieu, E., 1991. Breakage patterns of human long bones. J. Hum. Evol 21 (1), 27–48. https://doi.org/10.1016/0047-2484(91)90034-S.
Villa, P., Roebroeks, W., 2014. Neandertal demise: an archaeological analysis of the modern human superiority complex. PloS One 9 (4), e96424. https://doi.org/10.1371/journal.pone.0096424.
Handbook of the mammals of the world: lagomorphs and rodents I. In: Wilson, D.E., Mittermeier, R.A., Ruff, S., Martínez-Vilalta, A., Cavallini, P. (Eds.), 2016.
Wilson, D.E., Lacher, T.E., Mittermeier, R.A. (Eds.), 2017. Handbook of the Mammals of the World: 7. Rodents II. Lynx Edicions. Spain, Barcelona.
Wilson, D.E., Mittermeier, R.A., Ruff, S., Martínez-Vilalta, A., Cavallini, P., 2018. Handbook of the mammals of the world: insectivores, sloths and colungos. Lynx.
Wood, R.E., Douka, K., Boscato, P., Haesaerts, P., Sinitsyn, A., Higham, T.F., 2012. Testing the ABOx-SC method: dating known-age charcoals associated with the Campanian Ignimbrite. Quat. Geochronol 9, 16–26. https://doi.org/10.1016/j.quageo.2012.02.003.
Wood, R.E., Barroso-Ruíz, C., Caparrós, M., Pardo, J.F.J., Santos, B.G., Higham, T.F., 2013. Radiocarbon dating casts doubt on the late chronology of the Middle to Upper Palaeolithic transition in southern Iberia. In: Proceedings of the National Academy of Sciences, vol. 110, pp. 2781–2786. https://doi.org/10.1073/pnas.1207656110, 8.
Yravedra, J., 2004. Interacción de humanos y carnívoros en el Pleistoceno Superior de la Península Ibérica: novedosas interpretaciones en la cueva de Amalda. Espac. Tiempo Forma. Ser. Prehist. Arqueol 16–17. https://doi.org/10.5944/etfi.16-17.2003.4751.
Zilhão, J., Anesin, D., Aubry, T., Badal, E., Cabanes, D., Kehl, M., Matias, H., 2017. Precise dating of the middle-to-upper paleolithic transition in murcia (Spain) supports late neandertal persistence in Iberia. Heliyon 3 (11). https://doi.org/10.1016/j.heliyon.2017.e00435 e00435.